Nano Research 2017, 10(12): 4139–4174
DOI 10.1007/s12274-017-1763-4
Review Article
ISSN 1998-0124
CN 11-5974/O4

Recent advances in solid polymer electrolytes for lithium batteries

Qingqing Zhang[1], Kai Liu[2], Fei Ding[1] (✉), and Xingjiang Liu[1]

[1] *National Key Laboratory of Science and Technology on Power Sources, Tianjin Institute of Power Sources, Tianjin 300384, China*
[2] *School of Chemical Engineering and Technology, Tianjin University, Tianjin 300350, China*

Received: 23 April 2017
Revised: 8 July 2017
Accepted: 11 July 2017

KEYWORDS
lithium,
solid electrolyte,
polymer,
interfaces

ABSTRACT

Solid polymer electrolytes are light-weight, flexible, and non-flammable and provide a feasible solution to the safety issues facing lithium-ion batteries through the replacement of organic liquid electrolytes. Substantial research efforts have been devoted to achieving the next generation of solid-state polymer lithium batteries. Herein, we provide a review of the development of solid polymer electrolytes and provide comprehensive insights into emerging developments. In particular, we discuss the different molecular structures of the solid polymer matrices, including polyether, polyester, polyacrylonitrile, and polysiloxane, and their interfacial compatibility with lithium, as well as the factors that govern the properties of the polymer electrolytes. The discussion aims to give perspective to allow the strategic design of state-of-the-art solid polymer electrolytes, and we hope it will provide clear guidance for the exploration of high-performance lithium batteries.

1 Introduction

There is increasing demand for safe and energy dense batteries for use in consumer electrical devices, such as electric vehicles, portable devices, and smart grid community systems [1]. However, state-of-the-art lithium-ion batteries (LIBs) based on liquid electrolytes are inadequate for industrial applications [2–5]. Traditional LIBs offer volumetric and gravimetric energy densities of up to 770 $Wh \cdot L^{-1}$ and 260 $Wh \cdot kg^{-1}$, respectively. This bottleneck severely restricts the application of LIBs for large-scale energy storage equipment [6]. Consequently, it is now widely accepted that battery chemistries beyond liquid LIBs must be developed. Accordingly, there have been many efforts to address and develop alternative energy systems with higher energy densities and lower costs; for example, Li–S batteries and Li–O_2 batteries, which are the most promising next-generation energy storage systems, have ultrahigh energy densities [7, 8]. In this respect, lithium metal, which has the highest theoretical capacity (3,860 $mAh \cdot g^{-1}$ or 2,061 $mAh \cdot cm^{-3}$), lowest electrochemical potential (−3.04 V vs. the standard hydrogen electrode), and lowest density (0.59 $g \cdot cm^{-3}$) of studied materials, yields a very high electrochemical energy equivalent and represents the best choice of

Address correspondence to feiding_ncps@163.com

anode material [9, 10]. However, two major challenges must be addressed before the practical application of metal lithium to commercial batteries: Li dendrite growth and the low Coulombic efficiency after long-term charging and discharging. Lithium dendrites are the main cause of internal short circuits, thermal runaway, and sometimes even catastrophic failure. In conventional liquid electrolytes, although the growth of Li dendrites can be partially suppressed by the introduction of additives, this does not completely solve the safety issues facing lithium metal batteries [11, 12]. Furthermore, the low Coulombic efficiency leads to capacity fading during cycling because it is challenging to achieve sufficient passivation between the Li electrodes and the liquid electrolyte solution [13]. Regarding these issues, the formation of an Li-compatible physical barrier to suppress the dendritic growth is considered as a good strategy. However, the most promising strategy would be the replacement of conventional liquid electrolytes with a solid state electrolyte (SSE).

Compared with liquid electrolytes and gel polymer electrolytes, SSEs have two main advantages: (1) There is no leakage or flammability in an SSE and the formation of lithium dendrites in the anode can be mitigated, and (2) SSEs have longer cycle lives and require less packaging, enabling the operation of higher series voltages compared with those of liquid electrolytes. However, SSEs still have some drawbacks such as their complex manufacturing process, poor mechanical strengths, and large interfacial impedance, which remain the principal challenges preventing the manufacturing and fundamental understanding of SSEs.

SSEs can be divided into solid polymer electrolytes (SPE) and inorganic solid electrolytes (ISE) [6, 14]. Recently, a great many inorganic oxide electrolytes have been investigated extensively, such as NASICON-type phosphates [15], garnet oxides $Li_xLa_3M_2O_{12}$ (M = Ta, Nb, Zr) [16], and perovskite-type $Li_{3x}La_{2/3-x1/3-2x}TiO_3$ [17]. However, these oxide electrolytes with ionic conductivities up to 10^{-4} S·cm^{-1} at room temperature are still not sufficient to satisfy the requirements of real-world applications. The fabrication process is also complex. Sulfide electrolytes $Li_{10}GeP_2S_{12}$ and $70Li_2S$-$30P_2S_5$ glass ceramics with unprecedented conductivities of 1.2×10^{-2} and 3.2×10^{-3} S·cm^{-1}, respectively, have been reported [18, 19]. However, these sulfides can produce toxic H_2S on contact with moisture. Worst of all, they have low thermodynamic stabilities, being easily reduced by lithium metal and oxidized by high-voltage cathode materials.

Compared with ISEs, SPEs have several advantages: They are lightweight and flexible, have interfacial compatibility, and are very processable. Most importantly, they are very safe. SPEs are prepared by dissolving lithium salts in a high-molecular-weight polymer matrix. The polymer acts as the host for the transmission of lithium ions through the motion of polymer segments. More importantly, solid polymer-based electrolytes appear to be attractive as they can compensate for the volume changes of electrodes by elastic and plastic deformation [14]. SPEs, in general, are one of the most promising candidate electrolytes for all-solid-state Li metal, Li-ion, Li-sulfur, and Li-O_2 batteries [20, 21]. However, the ionic conductivities of SPEs are lower than the required conductivity of 10^{-3} S·cm^{-1}, limiting their practical use. The Bolloré Company have attempted to commercialize SPE-based lithium batteries, and Cui's group at the Qingdao Institute of Bioenergy and Bioprocess Technology have proposed a new generation of SPEs in recent years. Thus, SPEs have been studied by many groups globally, and the number of publications concerning SPEs has increased exponentially. Overall, this review discusses the advances in all-solid-state Li batteries based on SPEs from a unique perspective. It systematically describes the types of SPE according to the functional groups of the polymer matrix, including polyether, polyester, polyacrylonitrile, polysiloxane, and other polymers. In addition, factors affecting their compatibility with the anodic electrode and the remaining challenges for the future are summarized.

2 Theory of polymers in solid polymer electrolytes

2.1 Ionic conductivity

In an SPE system, the Li^+ cations are dissolved in the polymer solvents and are moved by the motion of the polymer chains. The number of free Li^+ cations and the moving ability of the chains significantly affects

the Li^+-transport ability within the SPE, in turn, influencing the performance of the batteries. A good understanding of the conducting mechanisms is favorable for the design and selection of polymer structures for the room temperature operation of solid polymer lithium batteries.

The conductivity, σ, of a material with multiple conducting species is governed by two parameters: The number of charge carriers and their mobility. The conductivity is given by Eq. (1)

$$\sigma = \sum n_i q_i \mu_i \quad (1)$$

Here, n_i represents the number of charge carriers of type i; q_i is the charge of the charge carriers, and μ_i is the mobility.

The ionic conductivity of the SPE systems often follows two dominant conduction mechanisms: The Arrhenius or Vogel-Tammann-Fulcher (VTF) equations, or a combination of these [22, 23].

The VTF equation can be derived from the quasi-thermodynamic models with the free volume and configurational entropy, and its behavior can be related to the ion motion coupled with the long-range motions of the polymer segments. This can be expressed by Eq. (2)

$$\sigma = \sigma_0 T^{-\frac{1}{2}} \exp\left(-\frac{B}{T - T_0}\right) \quad (2)$$

Here, σ_0 is the pre-exponential factor, which is related to the number of charge carriers n_i, B is the pseudo-activation energy of the conductivity, and T_0 is the reference temperature, which is normally 10–50 K below the experimental glass transition temperature.

The Arrhenius equation is shown in Eq. (3)

$$\sigma = \sigma_0 \exp\left(\frac{-E_a}{kT}\right) \quad (3)$$

Here, E_a is the activation energy, which can be calculated from the nonlinear least-squares fitting of the data from plots of $\log\sigma$ vs. $1/T$. For polymer electrolytes, plots of σ vs. $1/T$ are typically nonlinear, indicating that the conductivity mechanism involves an ionic hopping motion coupled with the relaxation and/or segmental motion of the polymeric chains [24].

A comprehensive description of lithium ion transportation in SPE is challenging because the systems are complicated and there is no simple structure–property correlation.

2.2 Glass transition temperature

The glass transition temperature (T_g) is one of the most important properties of polymers. It is the temperature at which the chain segments start to move while the molecular chains do not move. Below their T_g, there only exist the vibrations of molecule atoms or groups in their respective equilibrium positions. Below T_g, the polymers are rigid and brittle, and the molecules have very little mobility. At the T_g, a dramatic change occurs in the physical properties of the polymer host, including the density, specific heat, mechanical modulus, mechanical energy absorption, their dielectric and acoustical equivalents, and rate of gas or liquid diffusion through the polymer. Generally, T_g can be determined by differential scanning calorimetry (DSC) measurements. The polymer structure, crystallinity, molecular weight, thermal history, and pressure are considered to influence T_g.

Generally, lowering the T_g can enhance the segmental mobility of the polymer chains, and this is the simplest and most efficient way to improve the ionic conductivity. Above T_g, the ions can move in the space provided by the free volume of the polymer host and migrate from one coordination site to a new site along the chains. Alternatively, the ions can hop from one chain to another under the effect of an electric field. Because the Li-ion conductivity in SPE at room temperature is low, strategies have been developed to lower the T_g and enhance the conductivity. In particular, the use of branched chains with lower T_g values compared to the host polymer chain and the addition of nano-additives are effective approaches to improve the ion transport capability of SPE.

2.3 Degree of crystallinity

Crystallinity is the extent of long-range order in a material and has a significant impact on the material properties. The crystallization of polymers is a process associated with the partial alignment of their molecular chains. Polymers can crystallize upon cooling from

the melt or solvent evaporation, corresponding to the different filming technologies used to fabricate polymer electrolytes.

The properties of polymers are determined not only by the degree of crystallinity but also by the size and orientation of the molecular chains. The degree of crystallinity can be estimated by different analytical methods including density measurements, DSC, X-ray diffraction (XRD), infrared spectroscopy, and nuclear magnetic resonance (NMR). In addition, the distribution of crystalline and amorphous regions can be visualized with microscopic techniques, such as polarized light microscopy and transmission electron microscopy [25].

The crystallization process involves nucleation and crystal growth. Nucleation starts with small, nanometer-sized areas where some chains or their segments align. These nucleation seeds can either dissociate or grow further depending on the conditions.

Apart from the thermal mechanism, nucleation is strongly affected by impurities, plasticizers, fillers, and other additives in the polymer. For this reason, the crystallinity can be reduced by the addition of inorganic particles or plasticizers into the polymer matrix. The SPE membranes are generally manufactured by the solvent casting method or a hot-press filming method, and the crystal growth is different between the melt and the solution.

2.3.1 *Crystal growth from the melt*

Crystal growth only occurs at temperatures below the melting temperature (T_m) and above T_g. Higher temperatures destroy the molecular arrangement, and, below T_g, the movement of molecular chains is frozen. Nevertheless, secondary crystallization can proceed even below T_g on the timescale of months and years.

The growth of the crystalline regions preferably occurs in the direction of the largest temperature gradient and is suppressed at the top and bottom of the crystalline lamellae by the amorphous folded parts at those surfaces. In the case of a strong temperature gradient, the growth has a unidirectional, dendritic character. In the preparation process, the working temperature (melt and post-processing temperature), retention time, pressure used in the hot-press method, material composition, and other parameters can be tuned to change the crystallinity and, consequently, the ionic conductivity of the polymer electrolytes.

2.3.2 *Crystal growth from solution*

Polymers can also be crystallized from a solution or upon the evaporation of a solvent. This process depends on the degree of dilution; that is, in dilute solutions, the molecular chains have no connections with each other and exist as separate polymer coils in the solution. Increasing the concentration, which can occur via solvent evaporation, induces interactions between the molecular chains and, possibly, crystallization, as in crystallization from a melt. The crystallinity can be controlled by several factors such as the concentration, solvent, additives, composition, solvent volatilization speed, and temperature.

Above all, the degree of crystallinity determines the mechanical and thermal properties, as well as the ionic conductivity, of the polymer. High crystallinity, which reduces ion transportation, decreases the free volume of the crystal because of the more compact packing of parallel polymer chains. In conclusion, favorable ionic conductivity can be obtained by lowering the degree of crystallinity by adding additives such as plasticizers, nanofillers, polymer blends, and grafted polymers.

2.4 Generic criteria for polymers

In rechargeable lithium batteries, the SPE acts as both the electrolyte and the separator, being sandwiched between the anode and the cathode. A polymer chosen for SPE should necessarily possess the following list of properties:

(1) Dissolution ability. There should be sequential polar groups such as –O–, C=O, and C≡N to dissolve lithium salts and form polymer-salt complexes.

(2) Electrochemically stability. There should be a wide voltage window with a large gap between the onset potentials for decomposition by oxidation and reduction.

(3) High ionic conductivities and ion transference numbers, as well as electric insulation, to sustain the expected performance and to minimize self-discharge process for extended storage life.

(4) Chemical and thermal stability. There should

be no chemical reactions during battery operation including within itself, with the electrodes, or with the current collectors and packaging materials used. Excellent thermal stability ensures the safety of the SPE-based batteries.

(5) Good mechanical strength. A high dimensional stability guarantees processing feasibility and the isolation of the positive and negative electrodes.

In addition to the above requirements, the SPE must meet other practical criteria for large-scale applications.

(6) Low cost.

(7) Sustainability: The use of abundant elements and a low impact synthesis.

(8) Low toxicity: Little pollution or few environmental hazards.

3 Polyether-based solid polymer electrolytes

Polyether, which has a sequential chemical structure of –C–O–C– groups, allows lithium salt dissociation and complexation, and the macromolecular flexibility of the backbone ensures sufficient ion dynamics [26, 27]. Among the polyether-based SPEs, poly(ethylene oxide) (PEO), has been widely used as a host for polymer electrolytes over the past few decades. Poly(ethylene glycol) (PEG) is chemically synonymous with PEO and refers to oligomers and polymers with low molecular weights (< 20,000). The shorter polymer chains result in good molecular mobility but are unfavorable to the mechanical strength of the SPE. Therefore, PEG is generally used either as a polymerization precursor or to modify inorganic fillers to enhance dispersion.

The study of PEO-based SPEs started after their discovery by Wright and coworkers in 1973 [28], and many reviews on the progress of these SPEs have been published since then. In 2015, Xie et al. presented a review of the developments and issues concerning PEO-based electrolytes for lithium-ion batteries and summarized the different approaches to reduce the crystallinity and, hence, to improve the ionic conductivity of PEO-based electrolytes, including blending, modifying, and making PEO derivatives. Herein, this review will discuss the typical results that have been reported in the last two years from a unique perspective.

As is well known, PEO easily forms a crystalline phase at room temperature. This hinders the lithium ion migration, which depends on the movement of polymer chains and occurs mostly in amorphous phases [29, 30]. Thus, PEO-based batteries usually operate at temperatures higher than the melting temperature of PEO, which is generally above 80 °C. However, the PEO homopolymer is a viscous liquid under these conditions and is mechanically too weak to mitigate the growth of lithium metal dendrites upon cycling [31, 32]. Many approaches have been explored to improve both the ionic conductivity and mechanical properties of PEO-based SPEs, including the use of nano-sized fillers and nanostructured block/grafted copolymers to promote the formation of localized amorphous regions [33, 34]. As shown in Figs. 1(b) and 1(c), the addition of nano-sized inorganic fillers or modification with block polymers can interrupt the ordered structure of the polymer matrix, enhancing the content of amorphous domain, thus facilitating the transfer of lithium ions [35–38].

3.1 Nano inorganic fillers

Nanofillers provide a higher surface area that allows efficient contact with the electrolytes, enhancing the cell capacity, shortening the lithium diffusion pathways, and facilitating the lithium insertion–extraction reactions as compared to their conventional bulk counterparts. Nanofillers, including nano particles and two- (2D) and three-dimensional (3D) ordered structures, have been prepared and investigated with respect to their

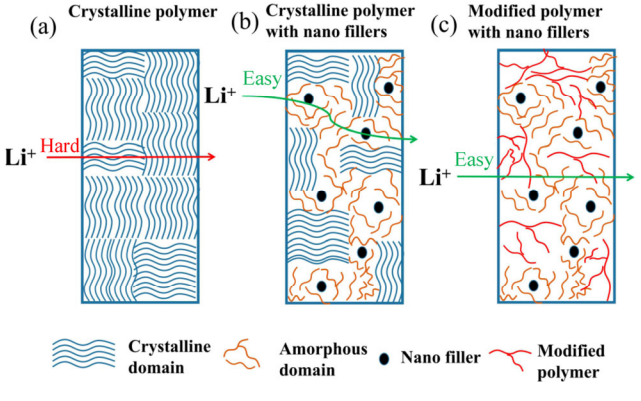

Figure 1 Schematic illustration of the lithium ion transfer across (a) a crystalline polymer, (b) crystalline polymer with nanofillers, and (c) modified polymer with nanofillers.

mechanical and electrochemical performance. It is believed that nano inorganic fillers can compensate for the deterioration in the mechanical properties that result from the low crystallinity of SPEs. Most importantly, these additives can often form pathways in the interphase for ion transportation, leading to improved ionic conductivity.

3.1.1 *Nanoparticles*

The addition of nanoparticles (such as SiO_2, Al_2O_3, and TiO_2) is believed to hinder the local reorganization of chains in the polymer and decrease the polymer crystallization, which favors high Li-ion transport. Meanwhile, many investigations have indicated that the Lewis acid-base model of interactions also supports the increased ionic conductivity, which is an interesting area and approach to improve electrochemical performance of composite polymer electrolytes [39].

Instead of simply mixing ceramic particles with polymers, Prof. Cui and his group introduced a novel synthesis of a SiO_2 filler inside the PEO polymer electrolyte. The *in situ* method further reduced the degree of polymer crystallinity, agglomeration of the nano fillers, and weak matrix–additive interactions, as shown in Fig. 2. As a result, high ionic conductivities of 4.4×10^{-5} S·cm^{-1} at 30 ℃ and 1.2×10^{-3} S·cm^{-1} at 60 ℃ were attained. Furthermore, the electrochemical stability window reaches 5.5 V vs. Li^+/Li. When used in the all-solid-state $LiFePO_4$/Li batteries, capacities of 120 and 100 mAh·g^{-1} were achieved at 90 and 60 ℃, respectively, and no significant capacity decay was observed within 80 cycles [40].

Another nanofiller, lithium aluminum germanium phosphate (LAGP), has been added to PEO and synthesized in the form of flexible hybrid SPE film [41]. It was found that the optimum composition of LAGP is 60 wt.%–80 wt.% in term of electrochemical performance, mechanical properties, and flexibility. The solid-state $LiFePO_4$/Li battery assembled with the as-prepared solid electrolyte (Fig. 3) delivered an initial discharge capacity of 137.6 mAh·g^{-1} and exhibited high capacity retention at 55 ℃. The composite solid electrolytes also showed good interfacial stability with the electrodes.

Tan et al. reported a new type of organic–inorganic hybrid PEO-based SPE, comprising a borane-doped PEG oligomer, nanosized Al_2O_3 particles, PEO, and lithium bistrifluoromethane sulfonimide (LiTFSI) [42]. This hybrid exhibits a lower T_g (–57.2 ℃) and melting point (41.6 ℃), as well as a higher ionic conductivity of 1.16×10^{-2} mS·cm^{-1} at room temperature, three times greater than that of the traditional PEO/Al_2O_3/LiTFSI membranes. The perfect properties arise from the dipole modification and higher free-volume space, which allows for significant Li-ion migration. When used in the lithium batteries, this hybrid presents remarkable reversible capacities (133 and 165 mAh·g^{-1} at 0.2C at 30 and 45 ℃, respectively), good rate capability, and stable cycle performance (141.9 mAh·g^{-1} at 0.2C at 30 ℃ after 150 cycles). This work shows that these novel hybrid electrolytes are promising candidates for future SPE-based lithium batteries. In addition, many other fillers have also been employed in PEO-based electrolytes to improve the SPE performance, such as $LiAlO_2$ [43–47], BN [48, 49], and $BaTiO_3$ [50–52].

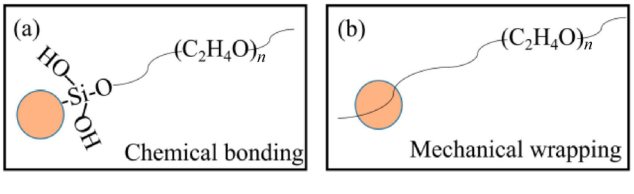

Figure 2 Two possible interaction mechanisms are shown, including (a) chemical bonding between the ends of PEO chains with hydroxyl groups on the modified SiO_2 surfaces and (b) mechanical wrapping of PEO chains during the growth of modified SiO_2 spheres.

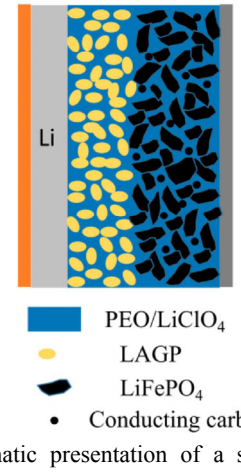

Figure 3 Schematic presentation of a solid-state $LiFePO_4$/Li battery assembled with hybrid solid electrolyte and the composite positive electrode.

3.1.2 *Nano 2D fillers*

Owing to its unique chemical and physical properties, graphene oxide (GO) has also been introduced into PEO-based SPEs for lithium battery applications, and these composites show nearly two orders of magnitude improvement in the ionic conductivity and a 260% increase in the tensile strength of the SPE with 1 wt.% GO content [53].

To increase the compatibility of GO with the polymer matrix, modification is necessary, and several different modification approaches have been used. Prof. Lee's group prepared PEG-grafted GO as the filler in a polymer matrix comprising a hybrid branched-graft copolymer based on poly(ethylene glycol) methyl ether methacrylate (PEGMA) and 3-(3,5,7,9,11,13,15-heptaisobutylpentacyclo-[9.5.1.1^{3,9}.1^{5,15}.1^{7,13}] octasiloxane-1-yl) propyl methacrylate (known as MA-POSS), as shown in Fig. 4. The ionic conductivity, thermal stability, and mechanical strength were dramatically improved because of the excellent dispersion of the functionalized GO in the polymer matrix and its ability to solvate the lithium ions. An all-solid-state V_2O_5/SPE/Li battery presented superior cycle performance compared to that of the pristine polymer matrix [54].

Ye et al. employed polymer-functionalized graphene to optimize composite polymer electrolytes (Fig. 5). The ionic transfer conditions, including Li salt dissociation, amorphous content, and segmental mobility, were significantly improved by the incorporation of 2D fillers. The ionic conductivity was enhanced by more than two orders of magnitude and 20-fold at 30 and 60 ℃, respectively. Furthermore, a 300% increase in the tensile strength (compared with the pure SPE) of the composite SPE was achieved with only 0.6 wt.% copolymer brush content. Furthermore, the SPE-containing battery exhibited a high capacity and long-term cyclic stability [55]. These results contribute to the development of high-performance SPEs for solid-state lithium batteries. Moreover, these investigations pave the way for gaining a better understanding of the role of structural design and tailoring the morphology of the SPE polymer matrix.

3.1.3 *Nano 3D fillers*

Halloysite nanotubes (HNT) are an aluminosilicate ($Al_2Si_2O_5(OH)_4$) natural nanoclay with a tubular 3D ordered structure and is one of numerous 3D nano resources. The inner and outer surfaces are oppositely charged [56]. A thin-film PEO/LiTFSI/HNT polymer electrolyte was reported by Lin et al., as depicted in Fig. 6. In this film SPE, lithium salts migrate into the ordered 3D channels in the electrolyte [57].

The interactions with the HNTs have been shown to enhance both the electrochemical and mechanical stability of the electrolyte. The ionic conductivity for the HNT/PEO-based SPE is 1.11 × 10^{-4} S·cm^{-1} at 25 ℃, and 2.14 × 10^{-3} S·cm^{-1} at 100 ℃. In this system, the lithium ion transference number reached 0.40. Furthermore, all-solid-state Li-S batteries prepared with the as-prepared electrolyte can operate at a wide temperature range from 25 to 100 ℃. At 25 ℃ and 0.1C, the battery presents stable discharge capacities with an average value of 745 mAh·g^{-1} over 100 discharge/charge cycles, a discharge capacity retention

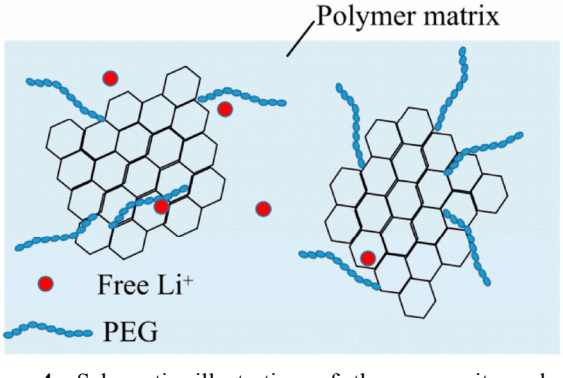

Figure 4 Schematic illustration of the composite polymer electrolyte containing the PGO filler.

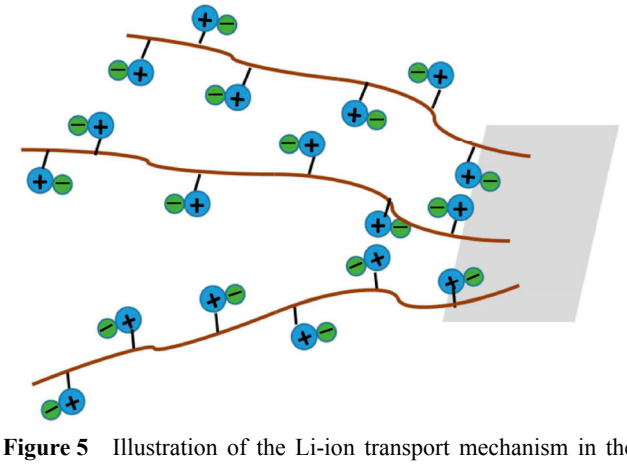

Figure 5 Illustration of the Li-ion transport mechanism in the PEO/Li$^+$/PIL(TFSI)-FG brush composite polymer electrolytes.

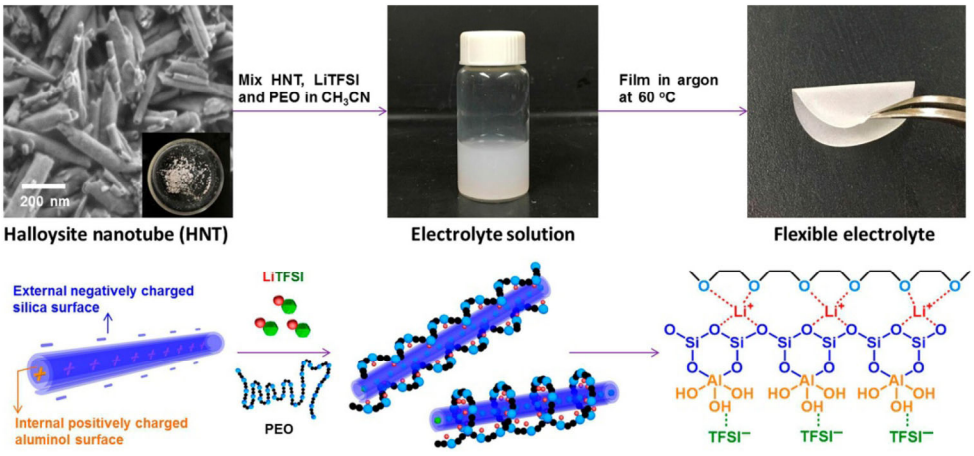

Figure 6 Preparation of HNT modified flexible electrolyte and mechanism of HNT addition for enhanced ionic conductivity. HNT, LiTFSI, and PEO are mixed in the solvent to form a uniform electrolyte solution. The solution is cast in an argon atmosphere to produce a flexible electrolyte thin film. Reprinted with permission from Ref. [57], © Elsevier Ltd. 2016.

of 87%, and close to 100% efficiency for each cycle. Even at 100 ˚C at a current rate of 4C, the battery delivers the discharge capacity of 809 mAh·g^{-1}. These results demonstrate the significant potential for the use of natural clay minerals in lithium batteries.

Prof. Lee from Nanyang Technological University presented a new kind of layer-by-layer self-assembly multilayer film consisting of PEG, an α-cyclodextrin (αCD) complex, and poly(acrylic acid) (PAA). The film is constructed via hydrogen bonding and supramolecular interactions [58]. The approach is a facile and efficient method to prepare SPEs with high ionic conductivities for electrochemical devices (Fig. 7). PAA limits the formation of a crystalline

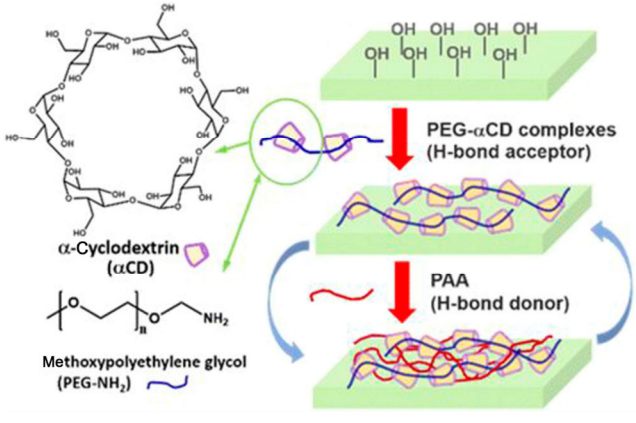

Figure 7 Schematic structure of the PEG-αCD complex structure and the layer-by-layer deposition process of PEG-αCD/PAA multilayer films. Reprinted with permission from Ref. [58], © American Chemical Society 2016.

phase in the PEG matrix, and the αCD forms nanochannels on the PEG backbone for lithium ion transportation. The 3D-structured filler αCD results in the tortuous chain packing of PEG and PAA because of steric effects. The PEG-αCD/PAA films show excellent performance, having ionic conductivities of 2.5×10^{-5} S·cm^{-1} at room temperature.

Pan et al. designed and prepared a new class of crosslinked SPE with 3D inorganic polyhedral oligomeric silsesquioxane (POSS) as the crosslinker and PEG as the lithium-ion solvating polymer using a simple one-pot reaction, as shown in Fig. 8 [59]. With the modification, the ion conductivity of the hybrid electrolytes at room temperature improves dramatically. In addition, the results demonstrate that the prepared SPE can resist lithium dendrite growth by tuning the crosslinked structures, even at high current densities. When cycled at 90 ˚C, the battery delivered a charge/discharge capacity close to the theoretical value of 170 mAh·g^{-1} for $LiFePO_4$ and showed no capacity decay for 50 cycles. The reported hybrid SPE is promising for the fabrication of next-generation, highly safe lithium batteries.

Metal-organic frameworks (MOF) are another type of 3D nanofiller for SPEs. These materials have inorganic-organic hybrid properties, high specific surface areas, and ordered microporous structures. These attractive characteristics have drawn attention for use as fillers to enhance the ionic conductivity and interfacial properties of SPEs, especially for the

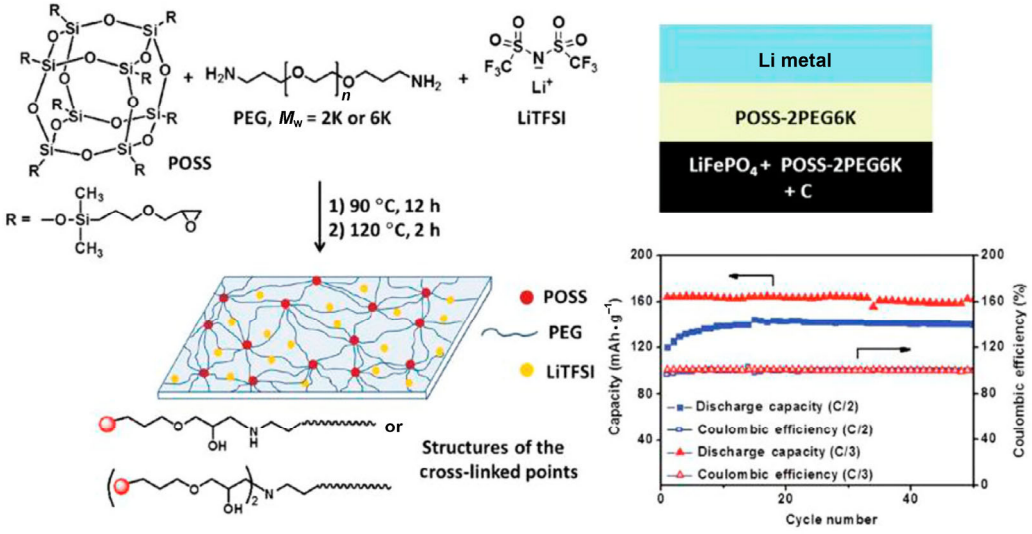

Figure 8 Synthesis of the POSS-PEG crosslinked SPEs. The geometry of the $LiFePO_4$/Li battery with $POSS\text{-}2PEG_{6K}$ as the electrolyte. Capacity and Coulombic efficiency vs. cycle number during galvanostatic cycling at C/2 and C/3 rates at 90 °C. Reprinted with permission from Ref. [59], © Wiley-VCH Verlag GmbH &Co. KGaA, Weinheim 2015.

PEO-based electrolytes. Zhang et al. used MOFs to modify the PEO/LiTFSI-based SPE in Li-S batteries [60]. The results demonstrate that the 3D additive has a positive effect on the battery performance by blocking polysulfide shuttling and dissolution. Kumar et al. incorporated a copper benzene dicarboxylate MOF into the PEO/LiTFSI electrolytes [61]. The ionic conductivity, compatibility, and thermal stability of SPE were improved after the addition of the MOF. In addition, the highly safe cell ($LiFePO_4$/SPE/Li) could even be cycled at 70 ˚C.

3.2 Copolymer electrolytes

Block/grafted copolymer electrolytes have recently been proposed as SPEs because these polymer structures suppress the crystallization of PEO and improve its mechanical properties. Generally, one of the copolymers is linear PEO, which acts as the ionic conductor, and the other is either the block providing the mechanical strength or a low-molecular-weight polymer grafted onto the backbone to increase the ionic mobility.

Bouchet and coworkers systematically analyzed the physicochemical and electrochemical properties of polystyrene–PEO (PS-PEO-PS) block copolymer electrolytes [62]. One block is a PEO-based polymer with dissolved lithium salts to impart ionic conductivity, and the PS block provides a membrane support for the electrolyte system. By varying the molecular weight and the composition of the copolymer electrolytes, the optimized electrolytes, together with a $LiFePO_4$ cathode, have been used to assemble lithium metal batteries. This battery operates at 40 ˚C, a temperature lower than the PEO melting temperature, where the PEO domains are partially crystallized. The batteries using such a block SPE architecture show very promising performance with good power retention, long cyclability at high C rates, excellent faradic efficiency, and good resistance to dendrite growth.

Diblock copolymers of poly(isoprene-b-ethylene oxide) and PI-b-PEO (IEO) have also employed as nanostructured polymer electrolytes doped with 1-ethyl-3-methylimidazolium trifluoromethanesulfonate ($CF_3SO_3{-}C_6H_{11}N_2$, EMITf) or lithium triflate (CF_3SO_3Li, LiTf), as shown in Fig. 9. The ionic conductivities in the two systems of IEO and PEO are fundamentally different. The lithium ionic conductivity of IEO/EMITf is much higher than that of the PEO/EMITf system. However, in IEO/LiTf, the conductivity is lower by a factor of a 100 relative to the PEO/LiTf case. The results reflect the critical influence of the lithium salts on the electrochemical performance, providing ways to manipulate the ionic motion in the polymer electrolytes [63].

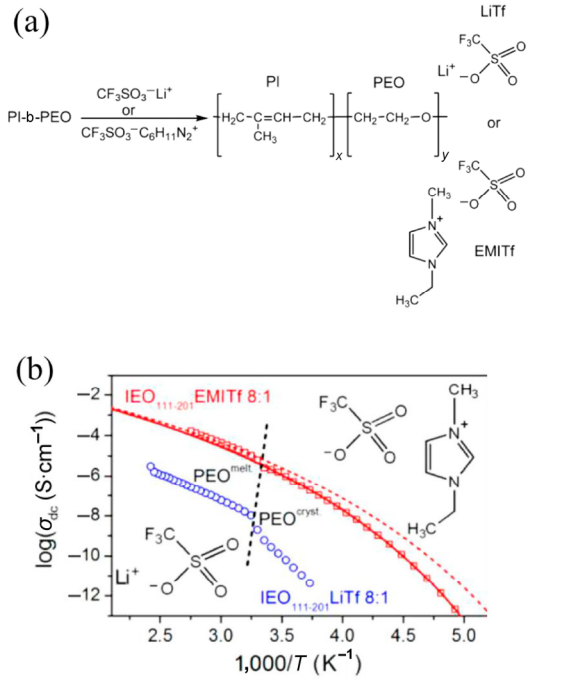

Figure 9 (a) Reaction scheme leading to the preparation of the block copolymer electrolytes. (b) D.C. conductivities for the polymer electrolytes as a function of temperature. Reprinted with permission from Ref. [63], © American Chemical Society 2015.

Porcarelli et al. designed an innovative polymer electrolyte system through a cost-effective and solvent-free *in situ* photopolymerization technique. The system comprises PEO as the SPE matrix, bis[2-(2-methoxyethoxy)ethyl]ether (tetraglyme, TEGDME) as the grafted molecule, LiTFSI as the source of lithium ions, and 4-methyl benzophenone (MBP) as the UV-induced photoinitiator (Fig. 10). Together with the oligomer additives, the SPE possesses robust mechanics, high flexibility, homogeneity, and is highly amorphous. Furthermore, the ionic conductivity at ambient temperature exceeds 0.1 mS·cm^{-1}, and electrochemical stability window is extended, reaching 5 V vs. Li/Li$^+$ (Fig. 10(b)). The solid polymer batteries show capacity retentions approaching 90% and Coulombic efficiency close to 100% (Fig. 10(c)). The electrolytes exhibit lithium ion transference numbers of 0.61 and have good interfacial compatibility with the lithium electrode and resistance to dendrite growth. This opens a new approach for the next generation of all-solid lithium-metal batteries that operate at ambient conditions [64].

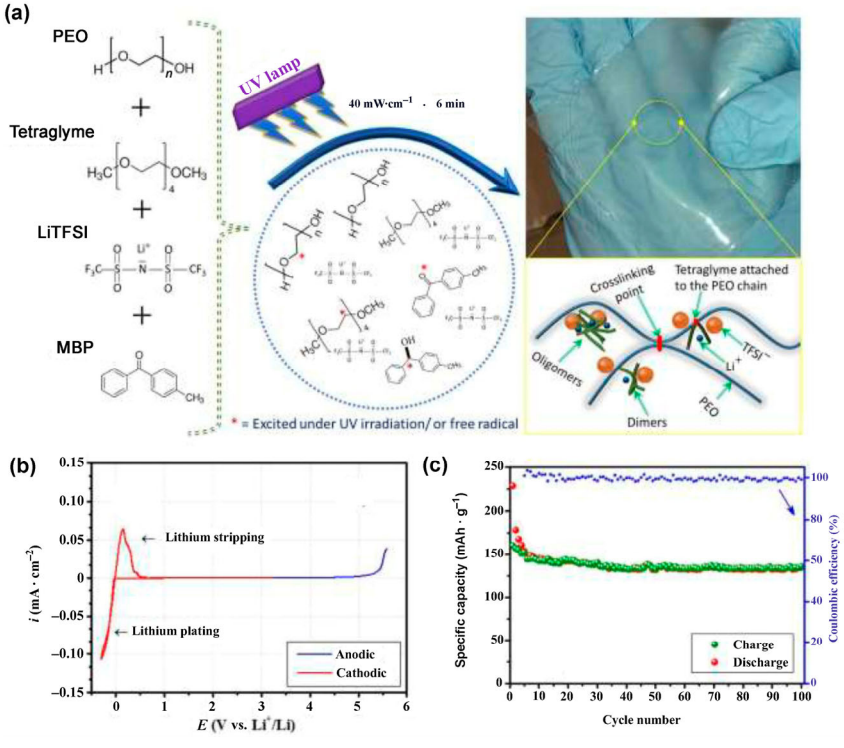

Figure 10 (a) Sketched representation of interlinked solid polymer electrolyte (ISPE) preparation along with used materials, and an illustration (right bottom) of the proposed interconnected PEO chains with hypothesized branched clusters of tetraglyme oligomers. In the top right, the real aspect of a freshly prepared ISPE. (b) Electrochemical stability window (anodic and cathodic scan) of the electrolyte at 25 °C. (c) Graph illustrating the specific capacity vs. the number of cycles along with the Coulombic efficiency. Reprinted with permission from Ref. [64], © Nature Publishing Group 2016.

3.3 Single ion polymer electrolyte conductors

In addition to the ionic conductivity, the lithium ion transference number is another vital parameter for SPEs in lithium batteries. Low lithium ion transference numbers may cause the formation of a concentration gradient that generates significant osmotic forces, limiting the maximum power delivery during the charge-discharge process of the battery [65]. Various approaches for reducing the mobility of anions can significantly increase the Li^+ transference number. One common method is to anchor anions to the backbone of the single-ion conducting polymer electrolytes.

In a single-ion conductor, Li^+ has weak interactions with the anionic structure. This enables a high dissociation level and increases lithium ion transference number. Most single-ion conducting polymer electrolytes are structures of polyanionic, comb-like, network polymers and composites [66, 67]. Xue and his group have prepared a composite single ion SPE by blending lithiated poly(perfluoroalkylsulfonyl)imide (PFSILi) ionene with PEO (Fig. 11) [68]. This composite presented excellent electrochemical performance with a lithium ion transference number of 0.908, an ionic conductivity of 1.76×10^{-4} S·cm^{-1} at 80 °C, and an electrochemical window of up to 5.5 V vs. Li^+/Li. Compared to the traditional small lithium salt LiTFSI (a structure comparison is shown in Fig. 11(a)), PFSILi has a polyanionic structure, where the anions are anchored, preventing migration. On cycling the $LiFePO_4$/Li batteries, a reversible capacity of 140 mAh·g^{-1} at 80 °C was achieved, and 50 stable cycles were maintained for 1,000 h at 70 °C at a rate of 0.1C.

Ma et al. presented a novel single lithium ion conducting electrolyte composed of the lithium salt of a polyanion, poly[(4-styrenesulfonyl)(trifluoromethyl(S-trifluoromethyl-sulfonylimino)sulfonyl)imide] ($PSsTFSI^-$) and PEO, as shown in Fig. 12. The complex presented a transference number of 0.91, thermal stability of up to 300 °C, and lithium ion conductivity of 1.35×10^{-4} S·cm^{-1} at 90 °C [69]. These prepared single ion-conducting SPEs with excellent properties are considered to have a potential application in rechargeable lithium metal batteries.

3.4 Novel lithium salts

In addition to the polymer matrix, the properties of lithium salts also affect the performance of polymer electrolytes. Compared to traditional inorganic lithium salts such as $LiClO_4$, $LiAsF_6$, $LiBF_4$, and $LiPF_6$ [70], organic lithium salts containing sulfonate anions, such as lithium perfluoroethylsulfonate ($LiC_2F_5SO_3$), lithium perfluorobutylsulfonate ($LiC_4F_9SO_3$), and lithium triflate ($LiCF_3SO_3$, LiTf), have become the salts of choice because they are highly resistant to oxidation, thermally stable, non-toxic, and insensitive to ambient moisture [71, 72]. However, their ionic conductivity is low. To improve the ion pair dissociation effect, the lithium imide salts (LiTFSI) and lithium bis(perfluoroethyl-sulfonyl)imide ($LiN(C_2F_5SO_2)_2$, (LiBETI)) have been developed. These salts have larger anionic radii, which could result in higher Li^+ conductivity [73]. The major drawback of these lithium salts is that they corrode the current collectors, which makes them unsuitable for polymer electrolytes. Therefore, the search for more reliable lithium salts has remained a focus of investigation.

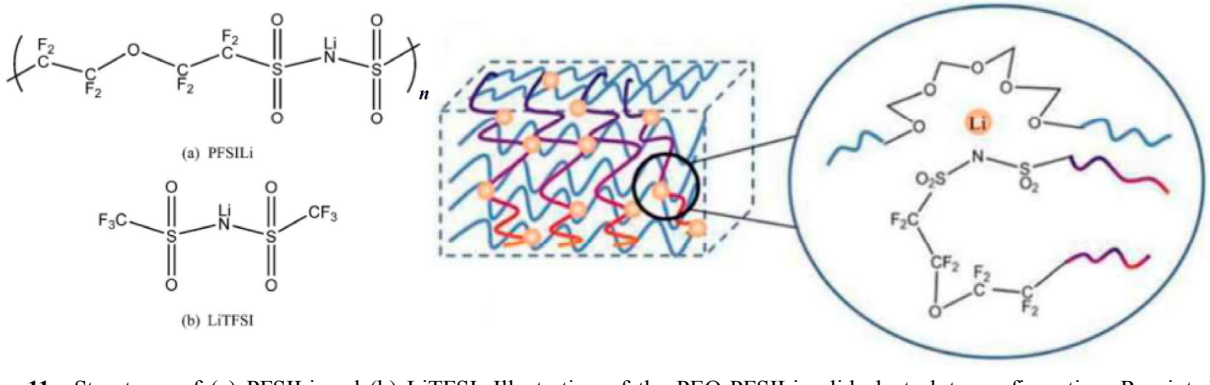

Figure 11 Structures of (a) PFSILi and (b) LiTFSI. Illustration of the PEO-PFSILi solid electrolyte configuration. Reprinted with permission from Ref. [68], © The Royal Society of Chemistry 2014.

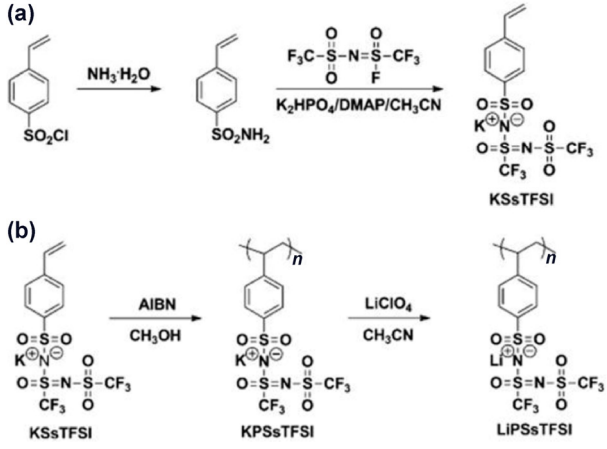

Figure 12 Synthetic routes of (a) monomer and (b) polymers. DMAP = dimethylaminopyridine and AIBN = azodiisobutyronitrile. Reprinted with permission from Ref. [69], © Wiley-VCH Verlag GmbH & Co. KGaA, Weinheim 2016.

Prof. Zhou and colleagues reported a novel SPE based on a perfluorinated sulfonimide salt. The SPE comprises lithium (trifluoromethanesulfonyl) (*n*-nonafluorobutanesulfonyl)imide (Li[(CF_3SO_2) (*n*-$C_4F_9SO_2$)-N], LiTNFSI) and PEO, which exhibits a relatively high ionic conductivity of 1.04×10^{-4} S·cm^{-1} at 60 °C and good thermal stability up to 350 °C. As shown in Fig. 13, the interface layer films between the LiTNFSI-based SPE and electrodes are compact and robust and significantly different from the loose and rough interfacial membranes in the LiTFSI salt. The interfacial impedance and morphology of the after-cycled lithium electrodes both proved that the LiTNFSI-based SPE could deliver excellent interfacial compatibility with lithium metal, which could inhibit the side reactions between the SPE and lithium. They demonstrated that this new lithium salt contributes to the development of high-energy all-solid-state lithium batteries [74].

A new class of dilithium (DL) salts from relatively inexpensive starting materials, whose structure is strikingly similar to LiTFSI, were developed by Chakrabarti et al. The imides are negatively charge on the nitrogen atom, and this charge is delocalized by two sulfone groups, resulting in highly mobile lithium ions, as shown in Fig. 14. In addition, a PEO-based film with the DL-1 salt exhibited an excellent ionic conductivity of 2.19×10^{-6} S·cm^{-1} at 30 °C [75].

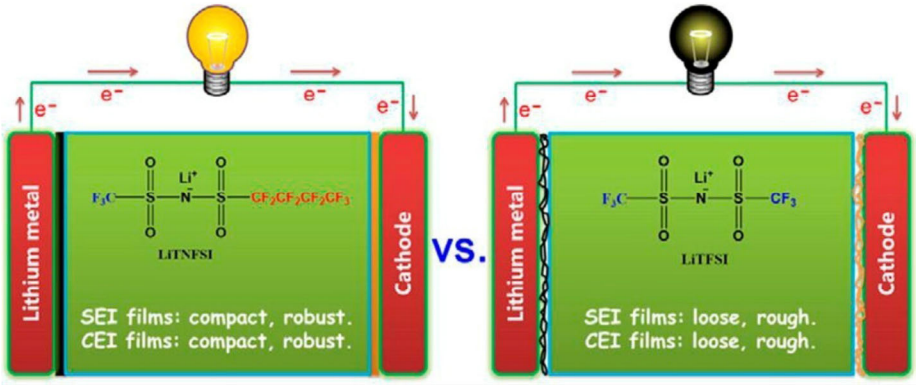

Figure 13 Schematic illustration of the formed interfacial films on the electrodes. Reprinted with permission from Ref. [74], © American Chemical Society 2016.

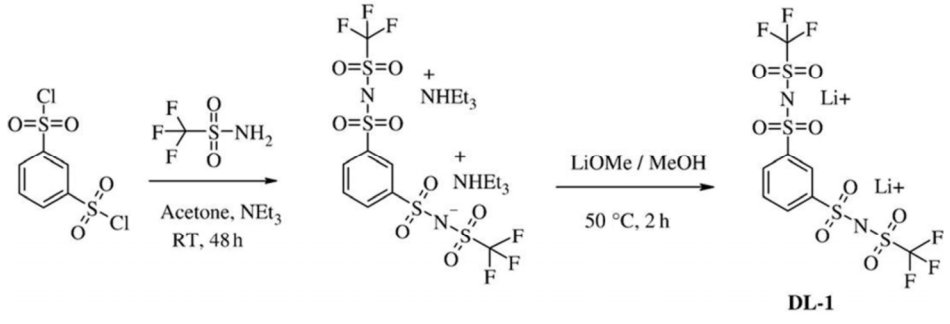

Figure 14 Synthesis of DL-1. Reprinted with permission from Ref. [75], © Elsevier B.V. 2009.

4 Polyester-based solid polymer electrolytes

Polyester-based SPEs have received considerable attention because of the strongly polar groups [–O–(C=O)–O–]. These polymers include polyethylene carbonate (PEC), poly(trimethylene carbonate) (PTMC), and poly (propylene carbonate) (PPC) (Table 1). They can efficiently dissolve alkali metal salts and reduce the tendency for the formation of ion aggregates. The sequential polar carbonate groups may enhance the dielectric constant and increase the ion conductivity in polymer electrolytes. Accordingly, polyester-based SPEs are a promising alternative for next-generation high-performance solid lithium batteries.

4.1 PEC

Jannasch and his group synthesized poly (ethylene oxide-co-ethylene carbonate) (PEO-EC) by the anionic ring-opening polymerization of ethylene carbonate (Fig. 15) [76]. Compared with PEO, PEO-EC, which incorporates polar carbonate groups into a polyether chain, not only reduces the crystallinity of the polymer but also increases the dielectric constant relative to polyethers with the same molecular weight. As a result, it provides the high flexibility necessary to promote ion mobility and is a promising polymer ion-conducting matrix for SPEs. A polymer having a number-average molecular weight of 2,650 g·mol^{-1} and an ethylene carbonate content of 28 mol% was selected to prepare a self-supportive SPE together with the LiTFSI salt. The ionic conductivity reached 6.3×10^{-6} S·cm^{-1} at 20 °C. According to Fourier transform infrared spectroscopy (FTIR) measurements, the lithium ions are coordinated by oxygen atoms in both the ether and carbonate groups, thus increasing the ionic dissociation.

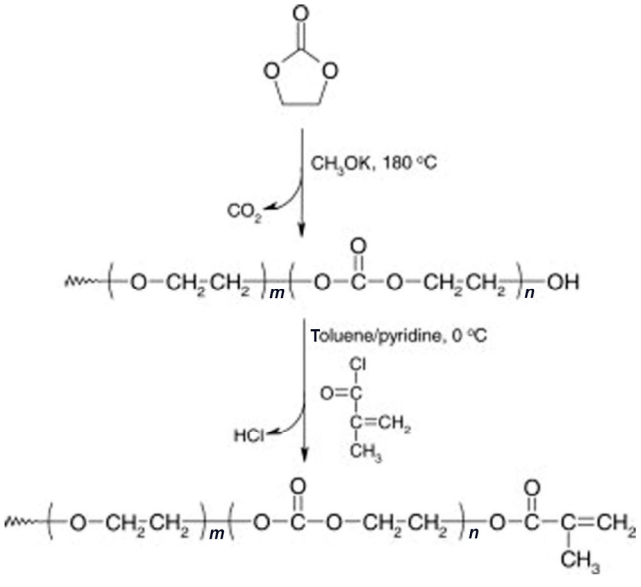

Figure 15 Synthesis of methacrylate-functionalized PEO-EC by the anionic ring-opening polymerization of EC, followed by the methacrylation of the terminal hydroxyl groups. Reprinted with permission from Ref. [76], © Wiley InterScience 2006.

Table 1 Properties of some typical polyester-based solid polymer electrolytes

Polymer	Chemical structure	T_g (°C)	T_m	Ref.
PEC	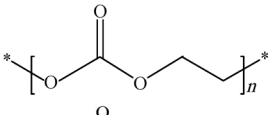	5	Amorphous	[76, 81]
PPC	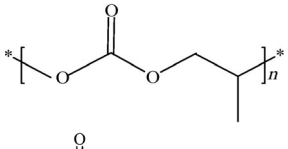	35	Amorphous	[79, 80, 98, 99]
PCL	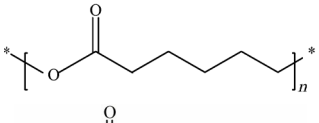	−60	Amorphous	[82, 83]
PTMC	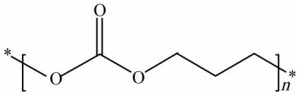	−16	Amorphous	[88–91, 94]
PTMC-PCL	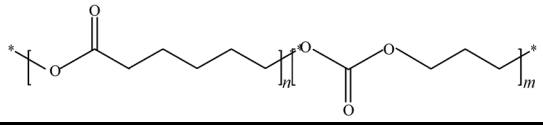	−28	Amorphous	[95, 96]

In 2014, Lee's group demonstrated an approach to synthesize a hybrid semi-interpenetrating network PEO-EC based SPE. It offers high ionic conductivity and sufficient dimensional stability for SPE applications through the incorporation of rigid and bulky octa-functional POSS acrylate (OA-POSS) and ethoxylated trimethylolpropane triacrylate, as shown in Fig. 16. The highest ionic conductivities achieved for this SPE were 3.74×10^{-5} and 3.26×10^{-4} S·cm^{-1} at 30 and 60 ˚C, respectively. The stable electrochemical window was up to 4.7 V at 60 ˚C. All-solid-state lithium batteries of V_2O_5/Li were fabricated by using of the prepared SPE, and the discharge capacity delivered by the cell was retained almost stably over 30 cycles. The composite SPE is considered to provide insight for the exploration of the PEO-EC polymer for future solid-state electrolytes [77].

The synthesis of PEC was first developed by Inoue and coworkers in 1968, motivated by the concept of CO_2 utilization [78]. In the case of a PEO based polymer electrolyte, the coupling of ether oxygen in the polymer framework and lithium ions is strong, so ion motion is difficult, and the lithium ion transference number is low. PEC, as a low-donor-concentration molecule, can reduce the coordinate bonding between the polymer chains and lithium ions in the polymer framework, thus increasing the ionic conductivity.

In 2014, Okumura investigated an SPE composed of PEC and LiTFSI. The Li^+ transference number of the PEC-based polymer electrolyte is 0.4, which is four times higher than that of a PEO based SPE (Fig. 17) [79]. According to the Raman spectra results, both the storage elastic modulus and T_g of the PEC-based SPE increase with increasing LiTFSI concentration up to 0.2 mol per repeating unit, possibly because of the coupling between the lithium ions and the polymer.

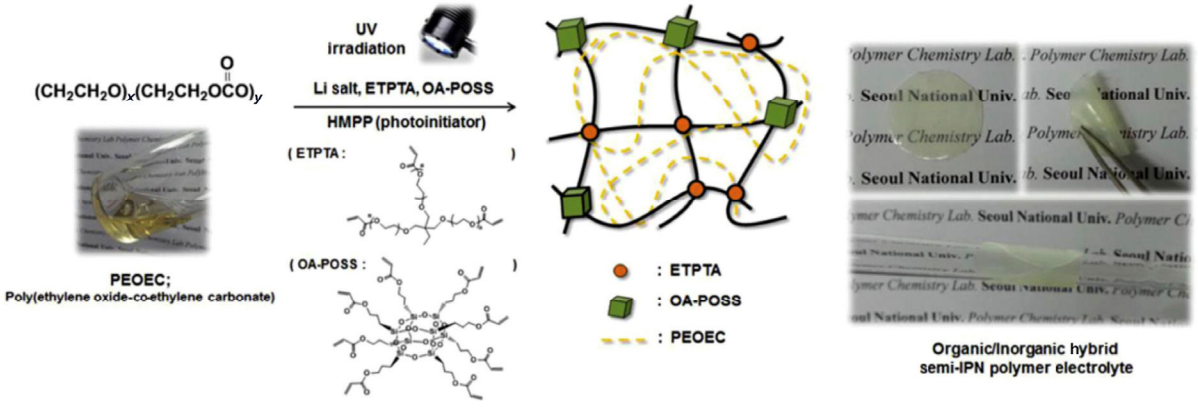

Figure 16 Preparation of organic/inorganic hybrid semi-IPN (semi-interpenetrating network) polymer electrolytes based on PEO-EC. Reprinted with permission from Ref. [77], © Elsevier Ltd. 2014.

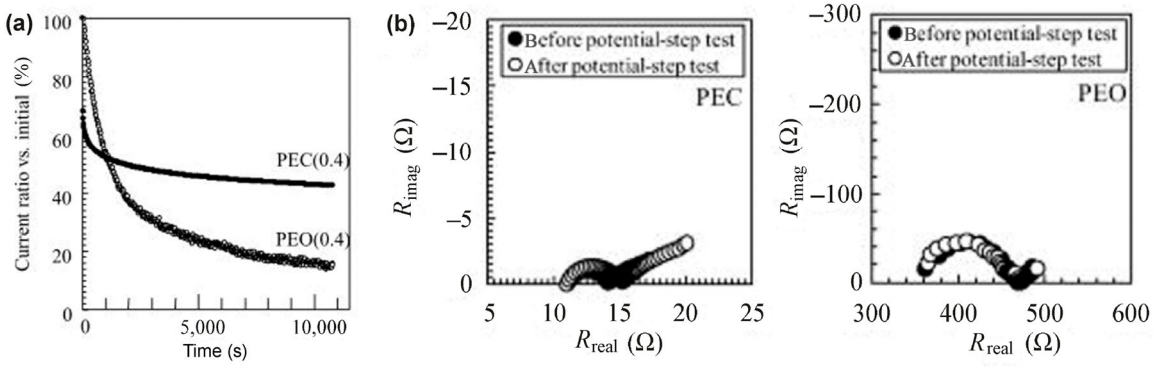

Figure 17 (a) Potential-step chronoamperometry and (b) impedance spectra variation before after the potential-step tests using a PEC-based polymer electrolyte and a PEO-based polymer electrolyte. The LiTFSI concentration is 0.4 per repeat unit of PEC or PEO. Reprinted with permission from Ref. [79], © Elsevier B.V. 2014.

However, because the abundance ratio of undissociated salt and the suppressed growth of the pseudo-crosslinks, the combination of a lithium salt with PEC at concentrations greater than 0.2 mol decreases both the storage elastic modulus and T_g of the polymer electrolyte. The highest obtained ionic conductivity of the PEC-based SPE was 0.47 mS·cm^{-1} at 20 °C.

Tominag et al. have found remarkable ion-conductive properties in polymer electrolytes composed of PEC and lithium bis(fluorosulfonyl) imide (LiFSI), and they investigated the relationship between the ionic conductivity and the salt concentration [38, 80]. Unlike the PEO system, with increasing lithium salt concentration, the ionic conductivity of the PEC/LiFSI electrolytes increases linearly, while the value of T_g decreases. In addition, the self-diffusion coefficient of Li^+ exceeded 10^{-7} cm^2·s^{-1}, and the lithium ion transference number was estimated to be more than 0.8 in composites with only 1 wt.% TiO_2 nanoparticles. In this system, ionic conductivities of 5.6×10^{-5}, 2.2×10^{-4}, and 4.3×10^{-4} S·cm^{-1} for the PEO_{20}LiFSI, $PEC_{0.53}$LiFSI (188 mol% of LiFSI), and $PEC_{0.53}$LiFSI-TiO_2 (1 wt.%)-based SPEs can be achieved, respectively. Polycarbonate is considered to be a superior SPE to polyether as an electrolyte matrix for use in flexible lithium batteries. Tominag et al. prepared a hybrid SPE membrane comprising PEC with 80 wt.% LiFSI in a 3D-ordered macroporous polyimide substrate with an average pore diameter of 0.3 μm and a thickness of 30 μm to assure the mechanical strength of the SPE. The acquired SPE had a conductivity of 1.6×10^{-5} S·cm^{-1} at 30 °C, a Li^+ transference number of over 0.5, and was electrochemically stable at more than 5 V vs. Li^+/Li. The reversible capacity of a $LiFePO_4$/Li coin cell containing this SPE reached close to 120–130 mAh·g^{-1} at C/20 rate at 30 °C, and delivered a reasonable capacity of 110 mAh·g^{-1} at a higher rate (C/10), as shown in Fig. 18. The cycle performance demonstrates that the prepared SPE could inhibit short circuit failures arising from lithium dendrites and mechanical instability. The use of a "pore-filling" technique, where functional PEC materials are added to the porous polyimide matrix, makes battery operation at ambient temperature possible in present all-solid-state batteries system. Thus, this work contributes to the development of flexible and safe energy device in future [81].

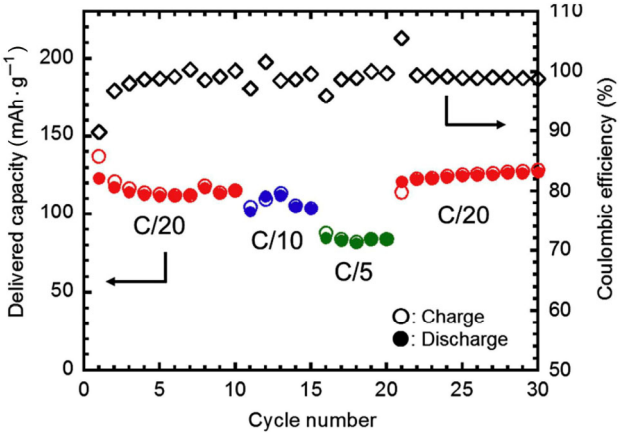

Figure 18 Delivered charge/discharge capacity and Coulombic efficiency of the Li/PEC-LiFSI/$LiFePO_4$ cell at 30 °C as a function of cycle number. Reprinted with permission from Ref. [81], © Elsevier B.V. 2016.

4.2 PCL

Polycaprolactone (PCL) is an environmental friendly polymer because it can be easily degraded in aqueous media and by microorganisms. In 2006, Fonseca et al. [82] provided the first report of a PCL-based SPE with different weight contents of $LiClO_4$. A maximum lithium ionic conductivity of 1.2×10^{-6} S·cm^{-1} was obtained at room temperature with 10 wt.% $LiClO_4$. In the composite system, complete biodegradation occurred after 110 days, which was attributed to the ester groups in the host polymer. The composite is electrochemically stable at approximately 5 V, demonstrating promise for the production of solid-state lithium batteries with low environmental impact. When a PCL-based SPE was applied to a rechargeable $LiNiCoO_2$/Li battery, specific discharge capacities of 182 mAh·g^{-1} in the first cycle and 120 mAh·g^{-1} after 50 cycles were obtained [83].

4.3 PTMC

PTMC is composed of repeated monomeric cation-coordinating units –(O=COCH$_2$CH$_2$CH$_2$O)–. It has been confirmed that PTMC can dissolve lithium salts and maintain ionic conductivity at a suitable level. In addition, it provides good thermal, mechanical, and electrochemical stability [84–87]. The lithium salts, including $LiBF_4$ [88], LiTFSI [89], and $LiPF_6$ [90], together with the amorphous host matrix PTMC, have received significant attention from many research

groups. The PTMC-based electrolytes have motivated the further development of this system for all-solid-state lithium batteries.

In 2014, Brandell's group synthesized high-molecular-weight PTMC to serve as a base polymer material for an SPE (Fig. 19) [91]. The thermal properties and ionic conductivity of polymer electrolytes with different salt ratios were measured by thermogravimetric analysis (TGA)/DSC and electrochemical impedance spectroscopy (EIS), respectively. The highest ionic conductivities, on the order of 10^{-7} S·cm^{-1} at 60 °C, were found in systems at [Li$^+$]:[carbonate] ratios of 1:13 and 1:8. The electrochemically stable window is up to 5.0 V vs. Li$^+$/Li. The $LiFePO_4$/Li half-cells with the electrolytes exhibited a plateau in the specific discharge capacity of 153 mAh·g^{-1} after long-term cycling, and the interfacial contact between the electrodes and the electrolyte films improved during cycling because of the softening of the electrolyte, in particular on the cathode side. In addition, unlike the aging principle in cycled Li-batteries with commercial liquid electrolytes at high temperatures, there was no capacity fading in the PTMC-based batteries during long-term storage and cycling for over 120 days at 60 °C [92, 93]. However, the PTMC SPE displayed a low initial discharge capacity, followed by a slow increase during storage/cycling, finally achieving the full capacity of the positive electrode after 70 days. To overcome this unexpected behavior, a highly viscous acetate-terminated PTMC oligomer was proposed as an interfacial mediator at the SPE/electrode interface [94]. This strategy not only helps to wet the interface between the electrode and the SPE without compromising the interfacial stability but also maintains the mechanical strength of the PTMC-based SPE. After this modification, the initial capacity of the battery was obviously improved. In addition, the cycling performances of batteries based on the SPE with different lithium salts were compared at elevated temperatures, and the long-term charge and discharge properties were demonstrated at different C-rates. Compared with polyethylene glycol dimethyl ether (PEGDME), batteries with the PTMC oligomer as an alternative interfacial mediator, display better capacity retentions and rate capabilities (Fig. 20). These results demonstrate that PTMC-based polymer electrolyte show promise for application in polycarbonate-based high-performance lithium batteries.

To increase the flexibility of the polymer chains and lower the T_g, thereby further increasing the ionic conductivity of PTMC-based SPE, Mindemark et al. substituted some of the TMC repeating units for CL because the T_g of the high-molecular-weight PCL is –60 °C, significantly lower than that of PTMC (–16 °C)

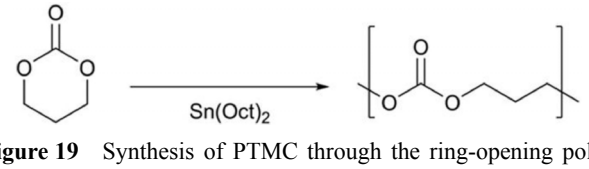

Figure 19 Synthesis of PTMC through the ring-opening polymerization of trimethylene carbonate catalyzed by tin(II) octoate. Reprinted with permission from Ref. [91], © Elsevier B.V. 2013.

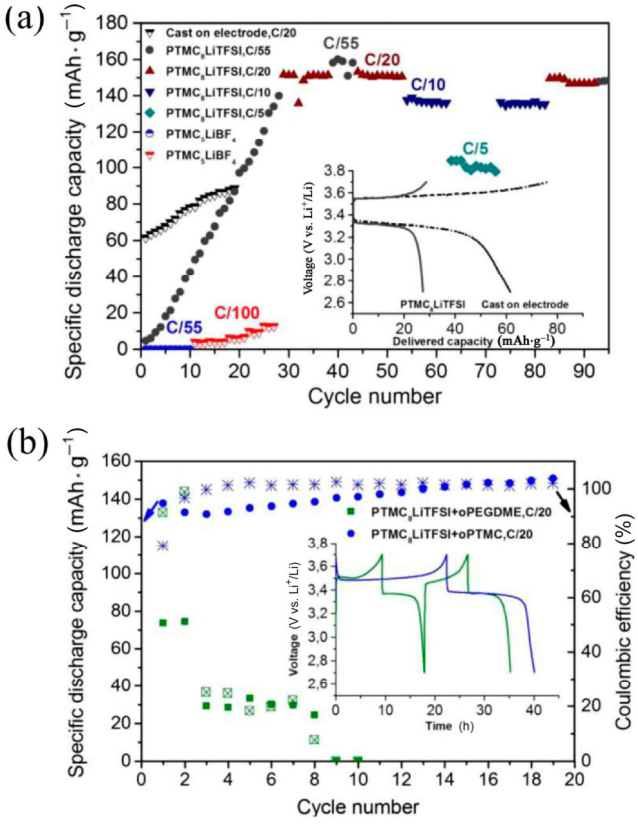

Figure 20 Cycling performance of Li/$LiFePO_4$ cells using (a) self-standing $PTMC_8LiTFSI$ or $PTMC_5LiBF_4$ compared to $PTMC_8LiTFSI$ directly cast onto the composite electrode (inset illustrating the cycling profile of $PTMC_8LiTFSI$ at C/20 during the 1st cycle). (b) Comparison of $PTMC_8LiTFSI$ using different oligomers (oPTMC or oPEGDME) at C/20 and 60 °C (solid dots for discharge capacity and stars for Coulombic efficiency). The inset shows the cycling profile during initial cycles. Reprinted with permission from Ref. [94], © Elsevier B.V. 2015.

(Fig. 21) [95, 96]. This permits their use in rechargeable solid lithium polymer batteries operating at ambient temperature. The best ionic conductivity achieved was 4.1×10^{-5} S·cm^{-1} at 25 ℃ and 1.1×10^{-4} S·cm^{-1} at 40 ℃ with 20 mol% carbonate repeating units. When cycled in Li/SPE/$LiFePO_4$ cells at room temperature, the specific capacity reached > 80% of the full capacity at C/50 and maintained about 60 mAh·g^{-1} even at C/10. The capacity was found to be excellent with no identifiable loss over 70 cycles (Fig. 22).

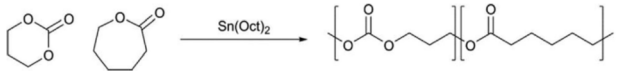

Figure 21 Synthesis of copolymers of trimethylene carbonate and ε-caprolactone. Reprinted with permission from Ref. [96], © Elsevier Ltd 2015.

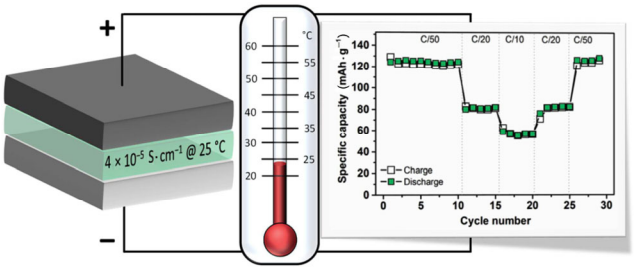

Figure 22 Geometry of the $LiFePO_4$/Li battery with PTMC-PCL as the electrolyte; Charge/discharge capacities and Coulombic efficiencies for a Li/SPE/$LiFePO_4$ cell with the electrolyte cycled at room temperature. Reprinted with permission from Ref. [95], © Elsevier B.V. 2015.

4.4 PPC

Poly(propylene carbonate) (PPC) is a biodegradable and regular alternating polyester, produced from propylene oxide and carbon dioxide in a heterogeneous catalyst system. PPC has attracted increasing interests as a promising host polymer for lithium batteries because of its amorphous nature, low cost, and green characteristics. PPC is believed to have an excellent ability to dissolve lithium salts and a good interfacial compatibility with electrodes, which arises from its similar chemical structure to the conventional carbonate-based liquid electrolytes [97, 98].

The 1-butyl-3-methylimidazolium tetrafluoroborate ($BMIM^+BF_4^-$) ionic liquid was added to the PPC/$LiClO_4$ SPE to improve the ionic conductivity, thermal and electrochemical properties, and safety [98]. As shown in Fig. 23, the composite polymer electrolyte forms a transparent, flexible, and self-standing membrane. The ionic conductivity of the electrolyte at room temperature is 1.5 mS·cm^{-1} with PPC/$LiClO_4$/$BMIM^+BF_4^-$ in a weight ratio of 1/0.2/3.

Cui and his colleagues, inspired by the traditional Chinese Taichi, exploited a rigid yet soft SPE combining nonwoven cellulose as the backbone and PPC as a polymer matrix for ionic transport [99]. The researchers, for the first time, produced an ambient-temperature all-solid-state lithium battery with increased safety at high-voltages using PPC as the solid polymer electrolyte. The study reveals a new perspective; that is, the high ionic conductivity of SPE is the result of low crystallinity and the appropriate glass transition temperature of the polymer electrolyte system. The cellulose PPC SPE had an ionic conductivity at 20 ℃ of 3.0×10^{-4} mS·cm^{-1}, one or two orders of magnitude higher than that of PEO-based SPEs over the temperature range from 20 to 120 ℃. At a high temperature of 120 ℃, the PPC-based SPE show an ionic conductivity of around 1.4×10^{-3} mS·cm^{-1} and perfect dimensional thermostability that could significantly improve the safety characteristics without the risk of internal short circuit. The wide electrochemical window of up to 4.6 V vs. Li^+/Li, demonstrates its potential for use in high-voltage lithium batteries. In addition, the electrolytes show excellent compatibility with lithium metal at room and elevated temperature. The specific

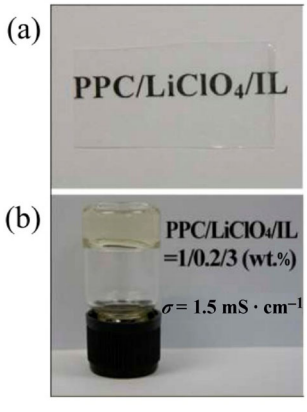

Figure 23 Photographs of PPC/$LiClO_4$/$BMIM^+BF_4^-$ electrolytes: (a) Transparent, flexible, and self-standing solid films. (b) Soft, sticky, and nonfluidic gel at the ratio of 1/0.2/3 (wt.%). Reprinted with permission from Ref. [98], © American Chemical Society 2013.

discharge capacity of the SPE-based $LiFePO_4$/Li battery at 20 ℃ was 142 mAh·g^{-1} at 0.1C and 52 mAh·g^{-1} at 3C, respectively. Even on cycling at 120 ℃, the cells showed improved safety characteristics and delivered a discharge capacity of 138.7 mAh·g^{-1} at 1C rate. The capacity retention was 95% after 500 cycles. Furthermore, when the SPE was used in a high-voltage $LiFe_{0.2}Mn_{0.8}PO_4$/Li cell, the charge and discharge curves exhibited flat profiles for the cathode and 96% capacity retention after 100 cycles. More importantly, the all-solid-state soft package assembled with the prepared SPE could power a red light-emitting diode lamp without internal short-circuit failures even after cutting away one part of the battery, as shown in Fig. 24. The study is a milestone in the research of room-temperature SPEs and motivates the development of all-solid-state lithium batteries for practical applications.

To further improve the unsatisfying ionic conductivity at ambient temperature to obtain a more reliable SPE, a free-standing and ambient temperature $Li_{6.75}La_3Zr_{1.75}Ta_{0.25}O_{12}$ (LLZTO)/PPC composite electrolyte was studied [100]. This composite has a high lithium ionic conductivity of 5.2 × 10^{-4} S·cm^{-1} at 20 ℃, a wide window of electrochemical stability of up to 4.6 V, a transference number of 0.75, and good mechanical strength of 6.8 MPa. The $LiFePO_4$ /Li batteries using the electrolytes have excellent rate performance (5C) and superior cycling stability (95%) at 20 ℃ (Fig. 25). Moreover, the PPC/LLZTO-based flexible $LiFePO_4$/$Li_4Ti_5O_{12}$ battery delivered the excellent electrochemical performance.

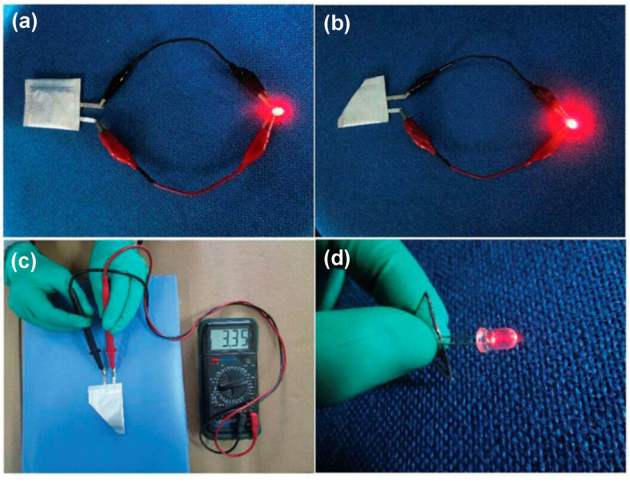

Figure 24 Illustration of the solid-state soft-package lithium cells (a) running well and (b) after cutting while powering a red LED lamp. (c) Voltage monitoring of obtained incomplete battery. (d) The obtained corner of the cell for lighting a LED lamp. Reprinted with permission from Ref. [99], © WILEY-VCH Verlag GmbH & Co. KGaA, Weinheim 2015.

With respect to PEO, Yu et al. for the first time incorporated PPC into a PEO-based electrolyte to decrease the glass transition temperature and crystallinity of PEO and to increase the lithium ionic conductivity [97]. The PEO/50%PPC/10%$LiClO_4$ SPE had a conductivity of 6.83 × 10^{-5} S·cm^{-1} at room temperature and showed no obvious decomposition up to 4.5 V vs. Li^+/Li.

To minimize the polarization caused by low lithium ion transference number, single-ion-conducting SPEs with anions anchored to the polymer backbone have been used to improve the transference number, as shown in Fig. 26. PPC-based single-ion-conducting polymer electrolytes with long flexible pendant groups of allyl glycidyl ether units were synthesized. The SPE has ionic conductivity of 1.61 × 10^{-4} S·cm^{-1} at 80 ℃, a high transference number of 0.86, and an electrochemical window up to 4.3 V [101].

5 Nitrile-based solid polymer electrolytes

Nitriles, which contain the polar and electron withdrawing group N≡C, have high dielectric constants of about 30. They also have a wide electrochemical window, probably because of the low lowest unoccupied molecular orbital (LUMO) energy. Recently, nitrile-based SPEs have received considerable attention because of their strong coordination ability and good electrochemical properties.

5.1 SN-based solid polymer electrolytes

Succinonitrile (N≡C–CH_2–CH_2–C≡N, SN) has a single plastic phase that extends from –35 ℃ to its melting point at 62 ℃ and a boiling point of 265 ℃. The dielectric constant of SN is 55 at 25 ℃, demonstrating that it has a strong ability to dissolve a wide variety of lithium salts. SN molecules can accept electrons and, thus, possess a high oxidation potential because of the lower LUMO [102], as shown in Fig. 27.

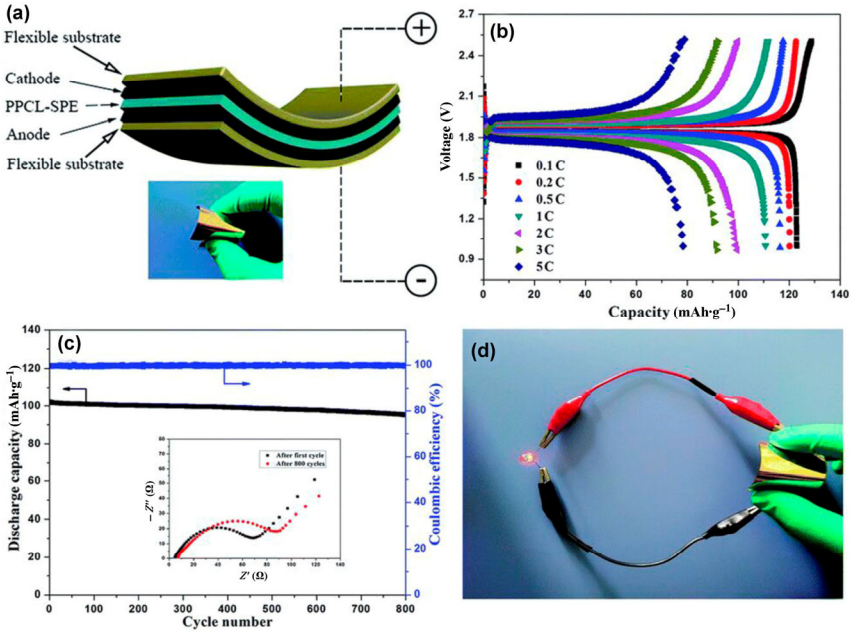

Figure 25 (a) Schematic of the flexible solid state $LiFePO_4/Li_4Ti_5O_{12}$ lithium-ion full cell. (b) Typical charge/discharge curves and (c) cycle performance of the solid state $LiFePO_4/Li_4Ti_5O_{12}$ lithium ion full cell. The inset is the impedance spectrum for the cell using PPCL-SPE after the first cycle and after 800 cycles. (d) Illustration of the flexible solid state $LiFePO_4/Li_4Ti_5O_{12}$ lithium ion full cell powering an LED lamp in a bent state. Temperature: 20 °C. Reprinted with permission from Ref. [100], © The Royal Society of Chemistry 2017.

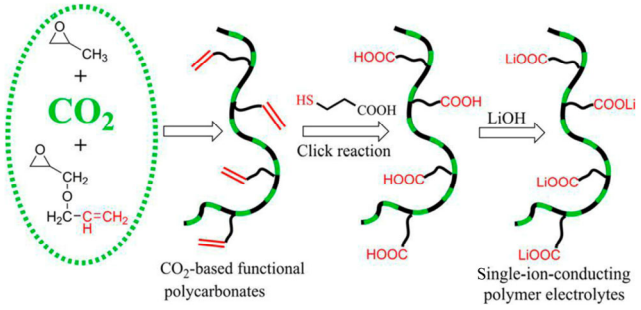

Figure 26 Illustration of synthesis process of PPC based single-ion-conducting polymer electrolyte. Reprinted with permission from Ref. [101], © American Chemical Society 2016.

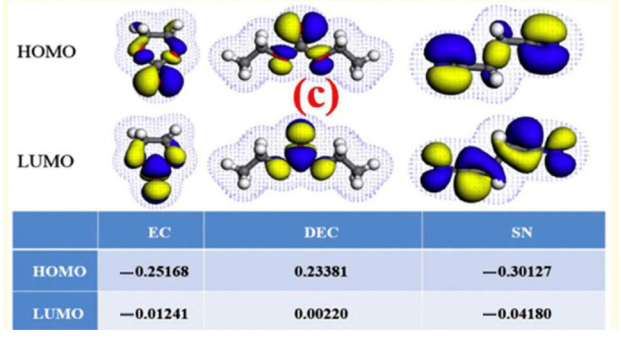

	EC	DEC	SN
HOMO	−0.25168	0.23381	−0.30127
LUMO	−0.01241	0.00220	−0.04180

Figure 27 Frontier molecular orbitals of EC, DEC, and SN and the energies of the occupied (HOMO) and unoccupied (LUMO) orbitals (in Hartree). Reprinted with permission from Ref. [102], © Elsevier B.V. 2015.

SN is a plastic crystal with a low molecular weight. In addition, it shows trans-gauche isomerism involving the rotation of molecules about the central C–C bonds. In 2004, Armand et al. found that the ionic conductivity reached 3 $S{\cdot}cm^{-1}$ for SN with a 5 mol% LiTFSI [103]. The plasticity of SN is similar to that of polymer electrolytes, indicating that the SN-based electrolyte can accommodate the volume changes that occur during the intercalation/deintercalation process of a lithium battery over long cycling periods. Unfortunately, the mechanical strength of the SN/lithium salt-based plastic phase electrolytes (PCE) is not sufficient for large-scale applications of lithium batteries. Therefore, SN is often combined with a polymer matrix to improve the mechanical properties of the composite, the so-called SN-based polymer electrolytes.

Lee's group discovered that, in contrast to a conventional plastic crystal composite electrolyte (F-PCCE) comprising polyvinylidenefluoride-co-hexafluoropropylene (PVdF-HFP) and PCE [104], the self-standing UV-cured ethoxylated trimethylolpropane triacrylate (ETPTA) polymer network films show strong mechanical strength and significant improvement in electrochemical stability and interfacial resistance toward lithium anode electrodes, as shown in Fig. 28.

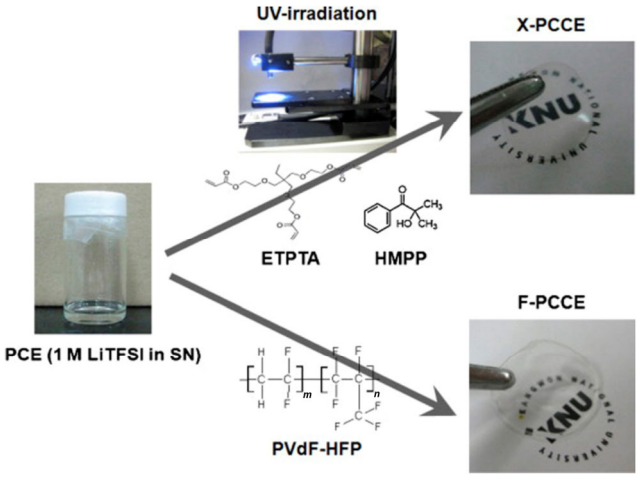

Figure 28 A schematic representation of the UV curing process and photographs of PCE, X-PCCE (ETPTA), and F-PCCE at room temperature. Chemical structures of ETPTA (UV-curable monomer), 2-hydroxy-2-methylpropiophenone (HMPP) (photo-initiator), and PVDF-HFP are also illustrated. Reprinted with permission from Ref. [104], © Elsevier Ltd. 2011.

In their subsequent work, the researchers proposed a bendable plastic crystal polymer electrolyte (B-PCPE) composed of SN, LiTFSI, and an ultraviolet-cured polymer network bearing trimethylolpropane propoxylate triacrylate (TPPTA) [105]. In comparison with the ETPTA polymer network (R-PCPE), the mechanical bendability of B-PCPE was significantly enhanced (Fig. 29), and the interfacial resistance between the B-PCPE and lithium metal electrodes was mitigated. In addition, B-PCPE presented a good cycling performance that is comparable to that of R-PCPE, presumably owing to its intimate interfacial contact with the electrodes during cycling.

In continuing efforts to develop advanced solid-state electrolytes for use in flexible lithium ion batteries, Prof. Lee et al. coated the UV-cured ETPTA on a porous, nonwoven polyethyleneterephthalate (PET) skeleton to obtain a 3D reticulated plastic crystal polymer electrolyte matrix, as shown in Fig. 30 [106]. They found that the ionic conductivity at 30 ℃ reached 5.7×10^{-4} S·cm^{-1}. A remarkable finding of this study was that the flexible $Li_4Ti_5O_{12}/LiCoO_2$ cell incorporating a PET-supporting SN electrolyte provided stable electrochemical performance without suffering from internal short-circuit problems in severely deformed states, even in a wrinkled state. The results facilitate the development of high-performance flexible energy storage system assemblies with advanced solid-state electrolyte alternatives to conventional liquid electrolytes.

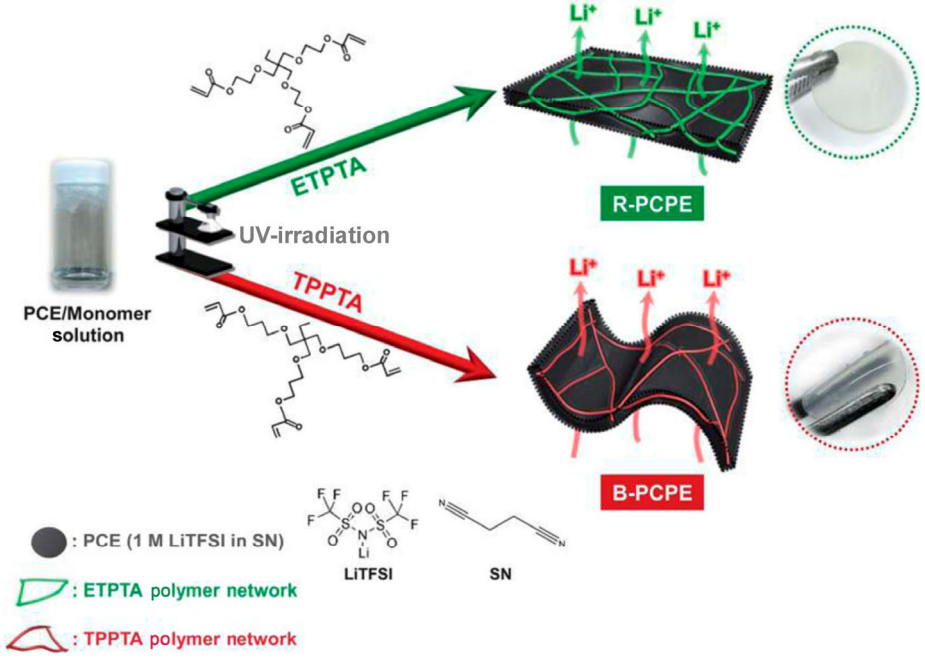

Figure 29 A schematic representation illustrating the UV-curing process and chemical structures of B-PCPE (UV-cured TPPTA polymer network/PCE) and R-PCPE (UV-cured ETPTA polymer network/PCE), along with their physical appearance. Reprinted with permission from Ref. [105], © The Royal Society of Chemistry 2013.

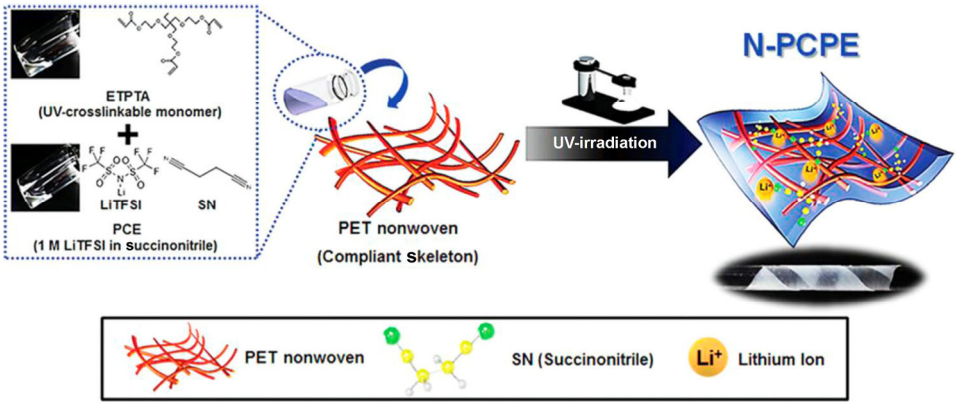

Figure 30 A schematic illustration of the UV polymerization-assisted fabrication process and chemical structure of N-PCPE (a new class of plastic crystal polymer electrolyte matrix combined with compliant PET nonwoven skeleton), along with a photograph showing the mechanical flexibility of N-PCPE. Reprinted with permission from Ref. [106], © WILEY-VCH Verlag GmbH & Co. KGaA, Weinheim 2013.

With the incorporation of Al_2O_3 nanoparticles, a satisfactory ionic conductivity of 1.02×10^{-3} S·cm^{-1} at room temperature was achieved because of the well-interconnected ion-conductive channels in the electrolyte systems [107]. Even after exposure to thermal shock, the self-standing composite film (plastic crystal composite polymer electrolyte, denoted as PC-CPE) remains dimensionally stable, with negligibly small areas suffering dimensional shrinkage (Fig. 31(a)).

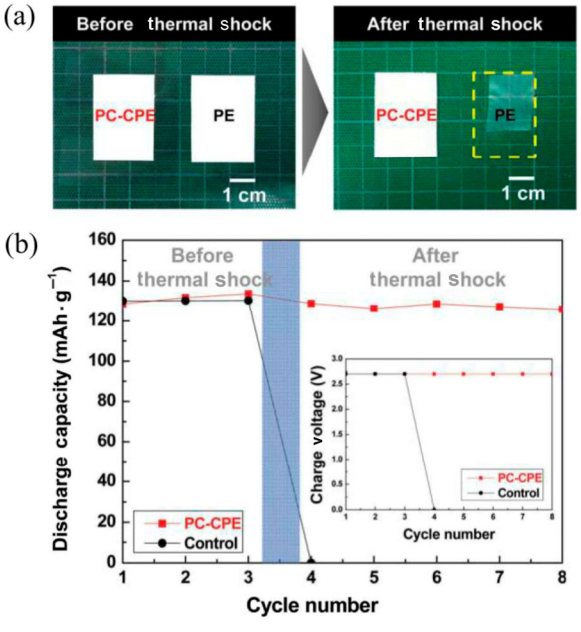

Figure 31 (a) Comparison of thermal shrinkage between the PC-CPE and PE separator after exposure to the thermal shock. (b) The variation in discharge capacity and charge voltage (inset) of cells before/after the thermal shock. Reprinted with permission from Ref. [107], © The Royal Society of Chemistry 2014.

Furthermore, the cell assembled with the membrane maintains stable charge/discharge performance (Fig. 31(b)).

In 2016, Liu et al. prepared vinyl-functionalized SiO_2 particles by the sol-gel method using triethoxyvinylsilane in an aqueous system (Fig. 32(a)) and investigated the effects of crosslinking the SN-based composite polymer electrolytes on the electrolyte properties [108]. Using Al_2O_3 additives effectively improves the thermal stability and interfacial compatibility between the electrolytes and electrodes (Figs. 32(b) and 32(c)) [109]. The composite electrolytes exhibit excellent performance in terms of their thermal stability above 230 °C, ionic conductivities, which reach 7.02×10^{-4} S·cm^{-1} at 25 °C, and electrochemical stability (up to 4.6 V vs. Li$^+$/Li). The $LiFePO_4$/Li cell presented superior cycle performance and rate capability, delivering a high discharge capacity of 154.4 mAh·g^{-1} at 0.1C after 100 charge–discharge cycles. Furthermore, the battery displayed a high discharge capacity of 112.7 mAh·g^{-1} at 2C rate, obviously higher than that of the cells assembled with previously reported polymer SN-based electrolytes.

5.2 Poly(acrylonitrile)-based solid electrolytes

Poly(acrylonitrile) (PAN)-based solid polymeric electrolytes have also been developed by many groups.

Rahman et al. discussed the influence of the TiO_2 filler concentration on the conductivity of the PAN/TiO_2/$LiClO_4$ electrolyte [110]. The addition of nanoparticles influences the ion motion in the polymer

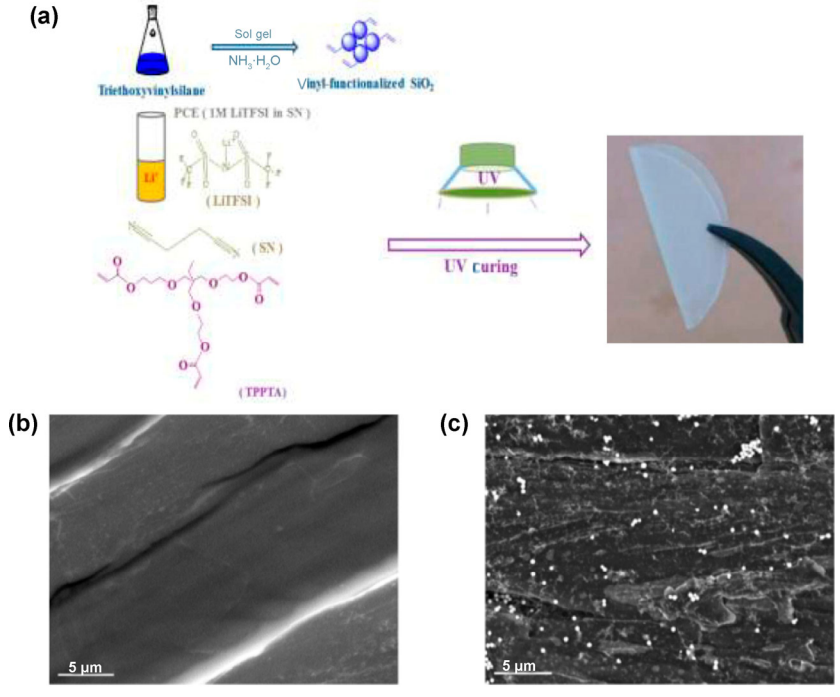

Figure 32 (a) The UV-curing process of SN-based polymer electrolyte. SEM images of lithium electrodes before/after 100 charge–discharge cycles. (b) Before charge–discharge cycling. (c) After 100 charge–discharge cycles. Reprinted with permission from Ref. [108], © American Chemical Society 2016.

matrix and lowers the segmental polymer dynamics. As the filler concentration decreases, the ionic conductivity increases and the glass transition temperature decreases significantly. The optimum conductivity of 1.8×10^{-4} S·cm^{-1} was obtained with 7.5 wt.% TiO_2.

The effects of the Al_2O_3 nanoparticles [111] on the ionic conductivity and transference number of a PAN/$LiClO_4$ electrolyte have also been investigated based on Lewis acid-base theory, as shown in Fig. 33. When the acidic Al_2O_3 ceramic is added (Fig. 33(a)), the polarizable nature of the lithium salts leads to the disassociation of the $Li^+ClO_4^-$ ion pairs, resulting in free Li^+ ions. At the same time, the stronger force of the H^+ on the acidic group than the Li^+ ions towards the nitrile group of PAN also free the nitrile-associated lithium ions. This increases the concentration of free Li^+ ions in the composite electrolyte, thereby enhancing the ionic conductivity. For basic Al_2O_3 (Fig. 33(b)), the interaction between the polar O atoms on the surface of Al_2O_3 and the Li^+ ions helps to reduce the interaction of both $Li^+ClO_4^-$ ion pairs and R–C≡N/Li^+ bonds, which free more ClO_4^- anions. The Li^+ ions interacting with polar O atoms can migrate near the filler grains. When neutral nanoscale Al_2O_3 is added (Fig. 33(c)), both interactions described above occur, and the anions can re-associate with the lithium ion cations to form new associates, lowering the concentration of charge carriers. These results indicate that the ceramic filler could also act as a source of charge carriers after suitable surface modification.

Chen-Yang et al. prepared a novel solid-state α-Al_2O_3-containing a PAN-based composite polymer electrolyte [112]. The researchers thought that the presence of nanofillers would reduce the free volume

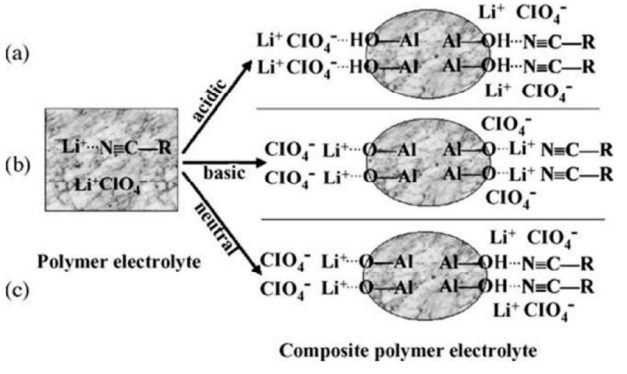

Figure 33 Schematic demonstration of the dissociation effects of (a) Lewis acidic, (b) basic, and (c) neutral surface groups on nano-Al_2O_3 particles. Reprinted with permission from Ref. [111], © Elsevier B.V. 2005.

of the material and the additive would act as a solid solvent to the salt in the composite rather than as a plasticizer. The highest conductivity of this composite was 5.7×10^{-4} S·cm^{-1} at room temperature, containing 7.5 wt.% α-Al_2O_3 and 0.6 $LiClO_4$ per PAN repeat unit. The stress-strain tests demonstrate that the as-prepared electrolyte films possess a high yield stress of 73 kg·cm^{-2}, indicating that the film is suitable for use as a separator in a solid-state battery. In addition, the high yield elongation of 225% indicates that the film is suitable for the formation of an excellent interface with the electrodes. Then, they prepared a series of nanocomposite polymer electrolytes based on PAN, $LiClO_4$, and a small amount of silica aerogel powder (SAP) prepared via the sol-gel method with an ionic liquid as the template [113]. The highest ambient ionic conductivity of the composite electrolyte is about 12.5 times higher than that without the addition of SAP, and a possible conduction mechanism is shown in Fig. 34. The electrolytes show excellent electrochemical stabilities and cyclabilities. At a rate of 0.5C, the discharge capacity was 120 mAh·g^{-1}, and the retained capacity ratio is 94.1% after 20 cycles.

To obtain free standing PAN-based thin films, poly(vinyl chloride) (PVC) was blended with PAN by a solution casting technique to improve the mechanical properties [114]. The polymer electrolyte with 30 wt.% LiTFSI has the highest ionic conductivity of 4.39×10^{-4} S·cm^{-1} at room temperature, and the thermal stability is up to 315 °C. The study expands the application of PAN-based SPEs in energy storage systems.

However, nitrile-based electrolytes undergo severe passivation upon contact with lithium metal anodes or lithiated graphite, and poor cathodic stability, which limits their further application. Modification strategies are expected to improve the properties of these composites, for example, the tailored structural design of polymer matrix and the addition of film-forming fillers embedded into the matrix framework.

Kang's group reported a novel polymerization of cyanoethyl polyvinyl alcohol (PVA-CN) materials through a greatly simplified approach, as shown in Fig. 35 [115]. The unique all-solid-state electrolyte is fabricated by the *in situ* polymerization of PVA-CN in the SN-based solid electrolyte that is filled with a network of PAN-based electrospun fiber membranes, which can greatly improve the mechanical strength of the as-prepared solid electrolyte and maintain it in a quasi-solid state without leakage even at temperatures greater than the melting point. Among these, LiTFSI was used as the lithium-ion provider because of its

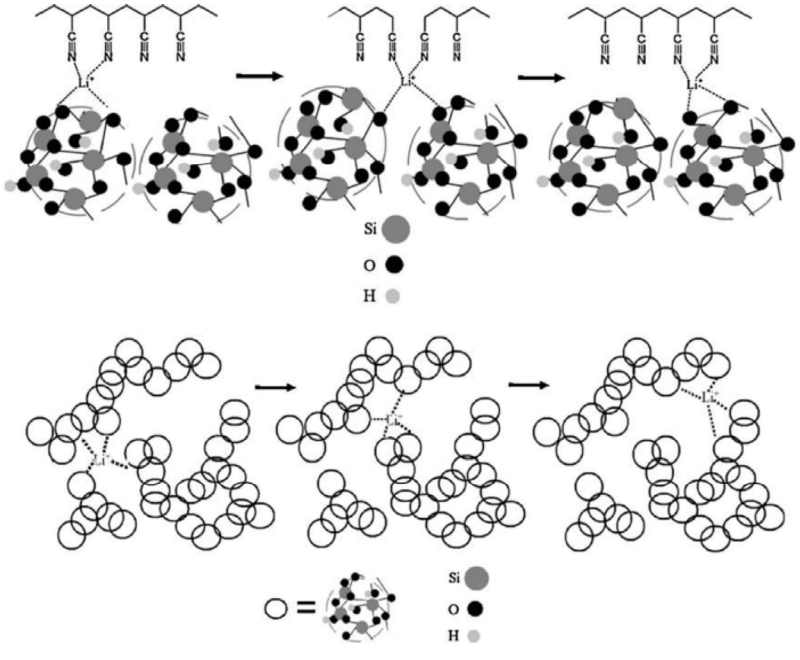

Figure 34 The proposed conduction mechanism of the lithium ion in PAN/SAP/$LiClO_4$ polymer electrolytes. Reprinted with permission from Ref. [113], © Elsevier B.V. 2010.

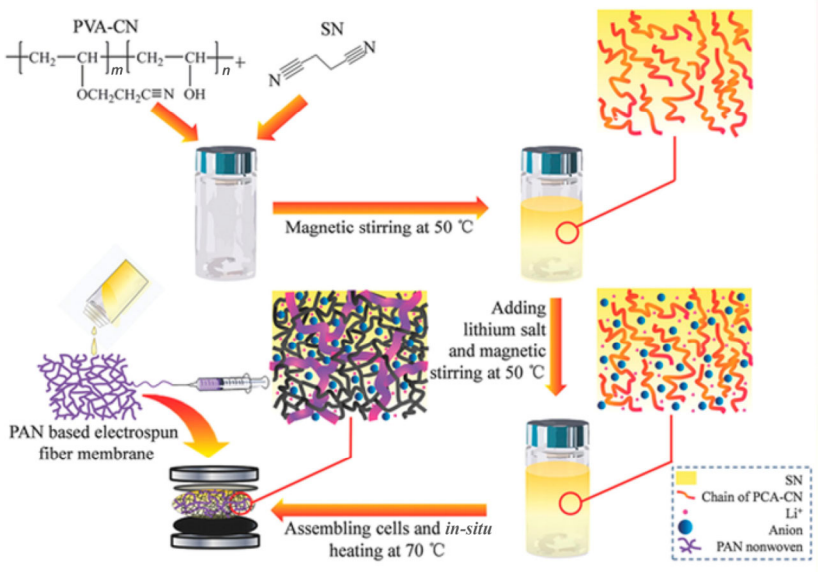

Figure 35 Schematic illustration for the *in situ* synthesis of the solid-state lithium battery. Reprinted with permission from Ref. [115], © WILEY-VCH Verlag GmbH & Co. KGaA, Weinheim 2015.

large anionic radius and low dissociation energy, thus improving the ionic conductivity. The initiator for polymerization of PVA-CN is PF_5, which is produced by the thermal decomposition of the lithium salt $LiPF_6$. The prepared film exhibits a high ionic conductivity of 4.49×10^{-4} S·cm^{-1}. Furthermore, the transference number is 0.57, and the film has a favorable mechanical strength of 15.31 MPa, excellent safety, and good flexibility. In addition, the film presents a satisfactory stability with aging and a superior compatibility with lithium metal electrodes. The $LiFePO_4$/Li cells, fabricated by *in situ* method, shows an initial discharge capacity of 154.6 mAh·g^{-1} at 0.1C, a Coulombic efficiency of 99.9%, and a capacity retention ratio approaching 96.7% after 100 cycles. During the rate performance tests, acceptable discharge capacities of 97.7 and 58.1 mAh·g^{-1} were achieved at 1.0C and 5C, respectively. Because of the superior performance and the simple fabrication process of the all-solid-state batteries, this is one of the most promising electrolyte materials for the next generation of lithium batteries.

6 Polysiloxane-based solid polymer electrolytes

Research into polysiloxane-based solid electrolyte started in the 1980s [116, 117]. These solid electrolytes have attracted considerable attention because of their exceptional thermal stabilities. Recently, most investigations have focused on the modification of the polysiloxane backbone by different methods. Li et al. tuned polysiloxane thin-film SPEs for all-solid-state batteries by the hydrosilylation of polymethylhydrosiloxane with cyclic [(allyloxy) methyl]ethylene ester carbonic acid and vinyl tris(2-methoxyethoxy)silane, as shown in Fig. 36. The as-prepared electrolyte had ionic conductivities of 1.55×10^{-4} and 1.50×10^{-3} S·cm^{-1}

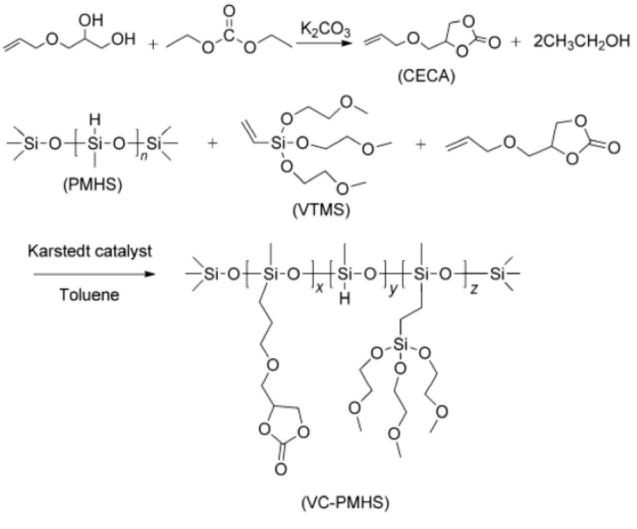

Figure 36 Synthesis of bifunctional polysiloxane. Reprinted with permission from Ref. [118], © WILEY-VCH Verlag GmbH & Co. KGaA, Weinheim 2014.

at 25 and 100 ˚C, respectively. The $LiFePO_4$/Li batteries assembled with the electrolyte showed excellent cycling performance at 25 ˚C. The results demonstrate that the structural modification of the polysiloxane-based electrolyte could markedly improve the performance of solid-state batteries [118].

Through a solvent casting method, three-dimensional hybrid inorganic-organic polymer electrolyte networks based on siloxane were prepared through a simple route (Fig. 37). High conductivities of up to 0.08 S·cm^{-1} were obtained at 30 ˚C. The thermomechanical and electrochemical stabilities are also very promising. The $LiFePO_4$/SPE/Li batteries deliver 85–90 mAh·g^{-1} at 60 ˚C and 0.1C without any capacity fading over 20 cycles [119].

In addition, a solvent-free hot-pressing method was also used to fabricate the crosslinked polysiloxane-based electrolyte through the reaction of $–OCH_3$ groups in 3-glycidoxypropyltrimethoxysilane and –OH groups in polyethylene glycol (PEG), as depicted in Fig. 38 [120]. The preparation process is low-cost and environmentally friendly. The prepared electrolyte demonstrated an ionic conductivity of 1.34×10^{-3} S·cm^{-1}, a decomposition window of 4.87 V at 120 ˚C, and thermal stability of up to 230 ˚C. The all-solid-state $LiFePO_4$/SPE/Li battery can work stably at temperatures of 80–140 ˚C, with an initial discharge capacity of 156.7 mAh·g^{-1} at 1C and 120 ˚C.

Natural food-grade starch [121], with –C–O–C– functional groups similar to the PEO structure, was crosslinked with γ-(2,3-epoxypropoxy) propyltrimethoxysilane to obtain a starch host SPE, as shown in Fig. 39. Thus, a novel SPE film using food grade starch as a host was fabricated. This electrolyte had

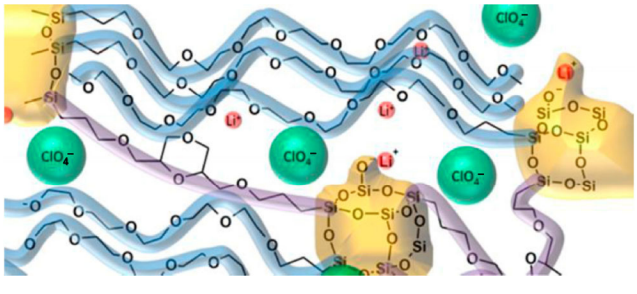

Figure 37 Schematic illustration of the preparation of the SPE. Reprinted with permission from Ref. [119], © American Chemical Society 2014.

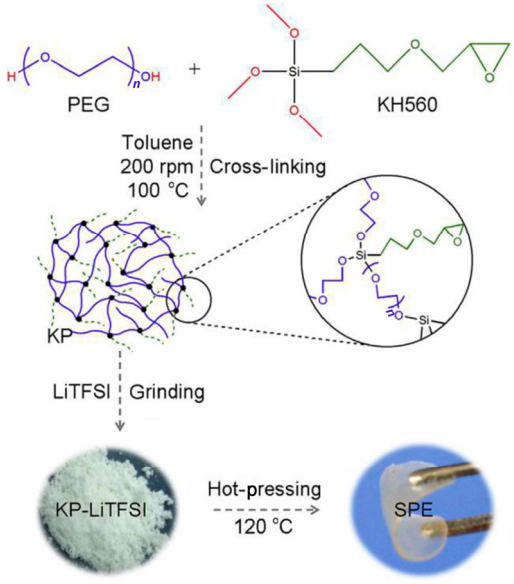

Figure 38 The preparation of KP-LiTFSI (KP, KH560-PEG powder) crosslinked SPE and photos of KP-LiTFSI powder and the SPE membrane made by a solvent-free hot-pressing method. Reprinted with permission from Ref. [120], © Elsevier B.V. 2015.

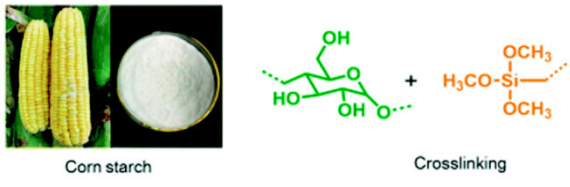

Figure 39 Scheme of the starch host synthesis. Reprinted with permission from Ref. [121], © The Royal Society of Chemistry 2016.

an exceptional ionic conductivity of 3.39×10^{-4} S·cm^{-1} and high transference number of 0.80 at 25 ˚C. The all-solid-state Li-S battery containing this low cost and highly sustainable electrolyte has an initial capacity of 1,442 mAh·g^{-1} and an average discharge capacity of 864 mAh·g^{-1} at 0.1C for 100 cycles at room temperature.

7 Others

The introduction of other polymer matrix-based SPEs means there is significant potential to enhance the performance of solid-state lithium battery. Besides the above-mentioned polymer electrolytes, a PVA-based SPE has also been explored for Li–air batteries, and this SPE has ionic conductivities extending from 10^{-4} S·cm^{-1} at room temperature to 10^{-3} S·cm^{-1} at 100 ˚C [122].

Poly[bis(methoxy-ethoxy-ethoxy)phosphazene] (MEEP), which has a low T_g, has also been investigated [123, 124]. This polymer remains completely amorphous at ambient temperature. MEEP can be crosslinked by gamma irradiation, and an MEEP-$LiCF_3SO_3$ electrolyte exhibited a room-temperature conductivity 2.5 orders of magnitude higher than that of PEO-based electrolytes [124]. Developing other new polymers with different functional groups is believed to be a reasonable strategy to obtain SPEs with sufficient performance to satisfy the criteria for the practical application of these devices.

8 Inorganic–organic hybrid polymer electrolytes

SPEs show high flexibility and have low fabrication costs, although they have some drawbacks including slightly inferior ionic conductivity ($< 10^{-5}$ S·cm^{-1} at room temperature), low Li^+ transfer numbers (≈ 0.3–0.6), and poor electrochemical stability at high voltages. For instance, the oxidative decomposition of PEO-based polymer electrolyte starts around 4.5 V vs. Li^+/Li [41]. ISEs have high ionic conductivities, are non-flammable, and have high Li^+-ion transfer numbers. However, they are brittle and have high interface resistance with the electrodes. Thus, hybrid solid-state electrolytes using polymer and inorganic solid electrolyte are expected to overcome the distinct disadvantages of ISEs and SPEs. Recently, Zhou's group prepared a hybrid solid electrolyte composed of poly(methyl methacrylate-styrene) (P(MMA-St)) and an amorphous ceramic, $LiNbO_3$, for an Li-O_2 battery (Fig. 40). These results provide an appealing strategy for the development of solid-state electrolytes. The prepared electrolytes offer excellent interfacial compatibility between the electrolyte and electrodes and can suppress the lithium dendrite growth to a certain extent. Furthermore, the solid-state Li-O_2 battery was shown to be stable after cycling for more than 100 cycles [125].

Cui and colleagues first incorporated ceramic nanowire fillers $Li_{0.33}La_{0.557}TiO_3$ (LLTO) into a PAN-$LiClO_4$-based solid electrolyte. The composite electrolytes exhibit an unprecedented ionic conductivity

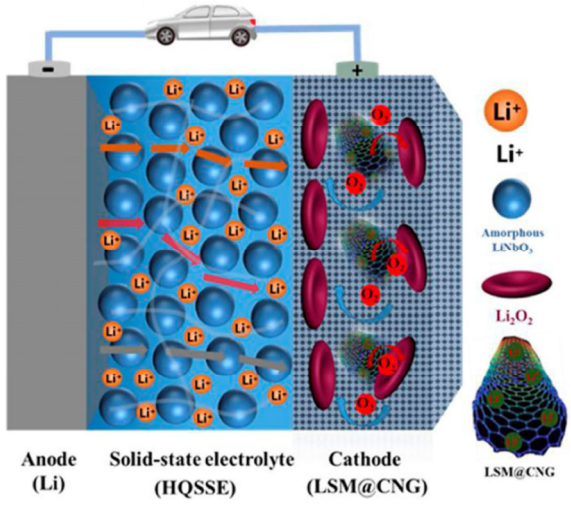

Figure 40 Schematic of the proposed hybrid solid electrolyte-based solid-state Li-O_2 battery. Reprinted with permission from Ref. [125], © Wiley-VCH Verlag GmbH & Co. KGaA, Weinheim 2016.

of 2.4×10^{-4} S·cm^{-1} at room temperature (Fig. 41(a)), which is attributed to the fast ion motion on the surfaces of ceramic nanowires and the formation of an ionic conductive network in the polymer matrix. The possible lithium ion conduction pathways in the nanowire-filled and nanoparticle-filled composite polymer electrolytes are also illustrated in Fig. 41(b). Furthermore, the composite SPE show an enhanced electrochemical stability window in comparison to the electrolyte without ceramic-nanowire fillers [126].

Composite solid electrolytes composed of $Li_{10}GeP_2S_{12}$ (LGPS) and PEO matrix have also been reported. The maximum ionic conductivity was 1.21×10^{-3} S·cm^{-1} at 80 ℃, and the electrochemically stable window is up to 5.7 V. The novel SPE demonstrates excellent compatibility with different electrodes ($LiFeO_4$/Li and $LiCoO_2$/Li). In addition, the $LiFePO_4$/SPE/Li battery shows attractive electrochemical performance with capacity retention of 92.5% after 50 cycles at 60 ℃ and capacities of 158 and 99 mAh·g^{-1} at current rates of 0.1C and 1C at 60 ℃, respectively. The results indicate the composite SPE is a promising candidate for solid state lithium batteries [127].

9 The interface between the SPE and anode

The SPE acts as both a separator and an ion conduction medium and possesses better chemical stability and

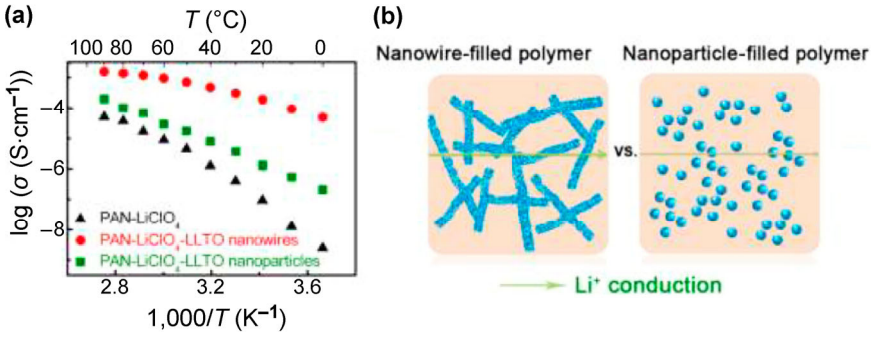

Figure 41 (a) Arrhenius plots of the composite electrolytes with and without LLTO nanowire, together with that of LLTO nanoparticle-filled electrolyte. (b) A comparison of possible lithium-ion conduction pathways in the nanowire-filled and nanoparticle-filled composite electrolytes. Reprinted with permission from Ref. [126], © American Chemical Society 2015.

enhanced safety compared to that of conventional liquid electrolytes. However, during battery charging, electron transfer from the anode electrode surface results in the decomposition of the electrochemically unstable components and salts near the electrode surface. As a result, a passive film on the electrode side is expected to form when the electrolyte contacts the lithium metal anode, as in liquid electrolytes.

An effective interphase layer should allow lithium ions to pass through and passivate the electrode surface to reduce undesirable and sustained side reactions drastically. The interphase layer has a decisive effect on the capacity retention, power capability, Coulombic efficiency, safety, and life span of the battery. Because of the rapidly growing interest in using intrinsically safe SPEs for large-scale lithium battery applications, a better understanding of the interface chemistry is urgently needed to improve the performance of all-solid-state lithium batteries. The importance of the interface layers between the electrolyte and the lithium electrode has been well recognized in academia and industry. In this section, the interphase layer characterization and its influence factors in SPE-based batteries will be reviewed in detail.

9.1 Solid electrolyte interphase characterization

The interface stability can be evaluated by several parameters, including the Li/polymer electrolyte interfacial resistance, the time evolution of the overall resistance of a symmetric Li/electrolyte/Li cell, as well as the electrochemical window, and the polymer electrolyte behavior during cycling.

Peled et al. detected the formation of a solid electrolyte interphase (SEI) layer on the lithium surface in PEO-based composite polymer electrolytes using EIS measurements (Fig. 42). They believed that the SEI resistance in battery electrolytes is typically in the range 10 to 1,000 Ω·cm^2. The results showed that the resistance at the grain boundaries for solid electrolytes is larger than the bulk ionic resistance near room temperature. The group proposed a model accounting

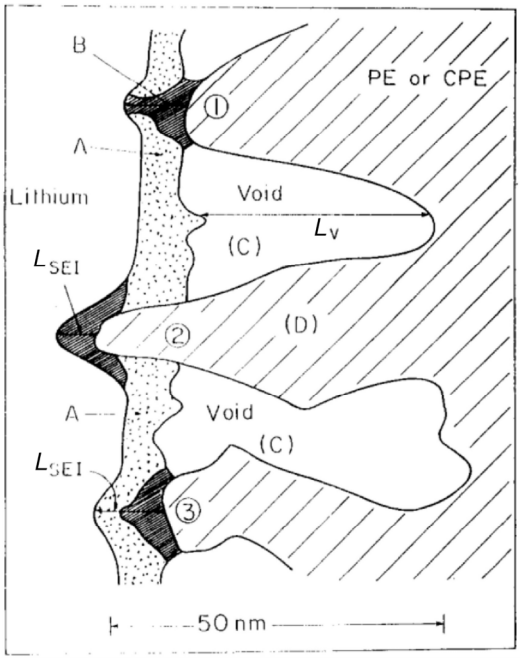

Figure 42 Schematic presentation of the Li/polymer electrolyte (PE) interphase: (a) Native oxide film, (b) freshly formed SEI, (c) void, and (d) polymer electrolyte (or CPE, composite polymer electrolyte). L_v = void height. Reprinted with permission from Ref. [128], © Elsevier Science Ltd. 1995.

for different types of Nyquist plots in the polymer electrolytes, but the technique did not allow for analysis of their compositions [128, 129].

Granvalet-Mancini et al. studied the SEI on lithium metal in contact with a PEO-triflate SPE through atomic force microscopy (AFM), attenuated total reflection FTIR spectroscopy, and A.C. impedance spectroscopy. The results indicate that one of the first reactions in the passivation process is the formation of CF_3 radicals, which abstract hydrogen atoms from the polymer backbone. Self-assembled molecular layers on the electrolyte surface are confirmed to help prevent the passivation reactions [130]. X-ray photoelectron spectroscopy (XPS) was also used to detect the surface layer and composition of lithium metal electrode after contact with an SPE containing LiTFSI or $LiBF_4$. The different lithium salts influence the film thickness, porosity, and resistance [131]. The formed layer consists of the decomposition product (LiF), salts, and the native film compounds Li_2CO_3/LiOH and Li_2O. Brandell et al. made a direct estimation of the composition of the interface layers by XPS [132]. There are obvious compositional differences in the interfaces formed by the PEO-LiTFSI systems and those of a liquid electrolyte (EC:DEC = 2:1, 1 M LiTFSI), as shown in Figs. 43(a) and 43(b). The moisture content in the polymer matrix is correlated with the formation of LiOH and, thus, played a critical role in the SEI composition. LiOH is considered to contribute to the increased interfacial resistance and the formation of protective layers on the active anode material.

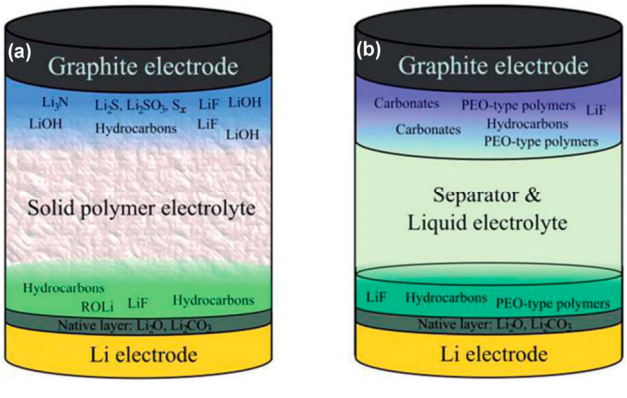

Figure 43 Schematic representation of the compositions of the SEI layers formed in (a) SPE-based and (b) conventional liquid electrolyte-based graphite half-cells. Reprinted with permission from Ref. [132], © The Royal Society of Chemistry 2014.

In the PTMC-LiTFSI systems [133], the SEI film close to the graphite surface is comparable to those observed in the water-absorbed PEO system. In contrast, the decomposition of the PTMC polymer host was observed at the interface of anode/SPE, and a proposed degradation mechanisms at low potentials is depicted in Fig. 44. The high content of LiOH found in hydrated PEO-based systems is not present in hydrophobic PTMC. At the $LiFePO_4$/SPE interface, good stability is believed to be irrelevant to the polymer host materials, with negligible amounts of LiF and salt decomposition products. Above all, the stabilization of the anode/SPE interface is crucial for the practical application of future all-solid-state lithium batteries.

9.2 Influencing factors

The resistance of the electrolyte/electrode interface is more than one order greater than that of the polymer electrolyte. Thus, it is necessary to control the interface performance to obtain high-performance SPE-based lithium secondary batteries.

Some factors influence the stability of the interface formed by PEO-based SPEs in contact with lithium metal electrodes. Passerini and his group investigated how the electrolyte preparation procedure, the filler additives, and the cell assembly process influence the interfacial properties of PEO-$LiCF_3SO_3$/Li cells [45]. First, the use of a completely dry host polymer of high-purity and a dry handling environment dramatically improve the performance of the Li/polymer electrolyte interface. Secondly, the addition of fillers in the composite SPE has a moderate effect on the interfacial compatibility of the electrolytes with the lithium electrode, when the preparation procedure and overall operating environment are optimized and controlled. The additives could suppress the reaction between lithium metal and salts. Finally, the battery assembly procedure is another critical factor for the establishment of an extremely stable interface film.

In addition, it was found that the species of lithium salts, LiX, also affects the interfacial stability of the Li/PEO-LiX system. The PEO electrolyte containing $LiClO_4$ exhibited a high interfacial resistance of 1,000 Ω·cm^2 at 70 °C for 25 days. In contrast, the resistance of interface between Li and SPE with

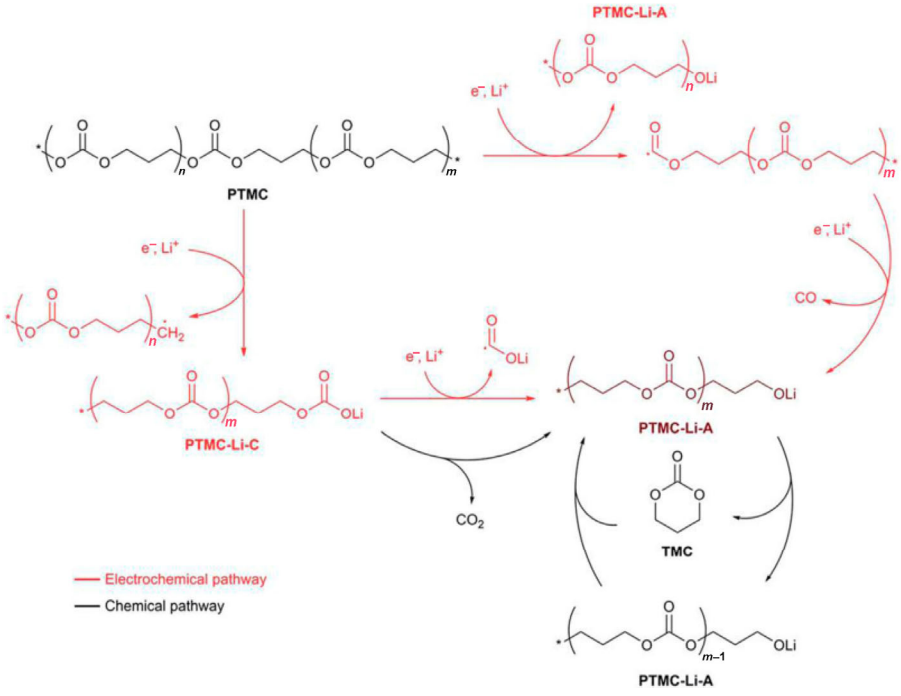

Figure 44 Schematic illustration of possible chemical and electrochemical degradation pathways of high-molecular-weight PTMC during electrochemical cycling. Reprinted with permission from Ref. [133], © The Royal Society of Chemistry 2015.

$Li(CF_3SO_2)_2N$ was as low as 67 Ω·cm^2 after storage at 80 °C for 30 days. After the addition of $BaTiO_3$ to the PEO-based electrolytes, the resistance was maintained at less than 50 Ω·cm^2 (Table 2) [134].

Bouchet et al. discovered that the evolution of the impedance spectra of symmetric lithium cells based on PEO-LiTFSI as a function of the aging time, temperature, and geometry of the electrolyte (of thickness

Table 2 Interfacial resistance of Li/PEO-LiX-filler/Li (R_{int}) and lithium ion resistance of polymer electrolyte films of 30-mm thickness (R_{Li}). Reprinted with permission from Ref. [134], © Elsevier Science B.V. 2001.

Electrolyte	Temperature (°C)	R_{int} (Ω·cm^2)	R_{Li} (Ω·cm^2)
PEO_8-$LiClO_4$	70	1,020 (25 days)	150
PEO_8-$LiClO_4$ 5 wt.% $BaTiO_3$ (1.8 μm)	70	380 (25 days)	17
PEO_8-$LiClO_4$ 1.4 wt.% $BaTiO_3$ (0.6–1.2 μm)	70	580 (25 days)	7
PEO_{12}-$Li(CF_3SO_3)$	85	140[a] (20 days)	64
PEO_{20}-$Li(CF_3SO_3)$	85	48[a] (20 days)	51
PEO_{20}-$Li(CF_3SO_3)$ 10 wt.% $LiNbO_3$ (1–5 μm)	85	47[a] (20 days)	30
PEO_{20}-$Li(CF_3SO_3)$ 20 wt.% $PbTiO_3$ (0.1 μm)	85	48[a] (20 days)	37
PEO_{20}-$LiBF_4$	85	348[a] (20 days)	17
PEO_{20}-$LiBF_4$ 5 wt.% $BaTiO_3$ (0.5 μm)	85	188[a] (20 days)	11
PEO_{19}-$LiPF_6$ 10 wt.% $BaTiO_3$ (0.5 μm)	80	120[a] (10 days)	150
PEO_{20}-$Li(CF_3SO_2)$2N	80	67[a] (30 days)	52
PEO_{20}-$Li(CF_3SO_2)_2N$ 10 wt.% $BaTiO_3$ (0.5 μm)	80	36[a] (30 days)	30
PEO_{20}-$Li(CF_3SO_2)_2N$ 1.5 wt.% $BaTiO_3$ (0.5 μm)	80	50[a] (10 days)	25
PEO_{20}-$Li(CF_3SO_2)_2N$ 10 wt.% $BTiO_3$ (0.1 μm)	80	54[a] (30 days)	25

[a] These cells were exposed to several cyclic voltammetry runs.

L and surface *S*) through EIS measurements [135]. By proposing an equivalent electrical circuit, the researchers gave a good explanation of the whole spectra, as shown in Fig. 45. The high-frequency domain ($f > 10^5$ Hz) corresponds to the bulk of the electrolyte, and the bulk resistance (R_b) does not depend on the aging time. The arc in the middle high-frequency domain (10^5–10^2 Hz) is generally due to the formation of a surface layer or/and the electronic charge transfer. The interphase capacitance (R_i) stabilizes after an aging period of 4 to 5 days. Finally, at low frequencies, the Warburg arc, which does not depend on aging, represents the transport of charged particles.

The molecular weight of PEO has an influence on the interface contact between the lithium anode and solid electrolyte [136]. PEO with different molecular weights (M_W = 6,000, 100,000, 500,000, and 900,000) and LiTFSI have been coated on the anode to guarantee the contact between the electrolyte and electrode surface. The results demonstrate that the crystallinity of PEO (LiTFSI) decreases with increasing PEO molecular weight. The PEO-500000-(LiTFSI) film modified on the anode possessed good mechanical properties and interfacial contact between the lithium anode and solid electrolyte. In addition, the materials provide a satisfactory cycling performance in a $LiMn_{0.8}Fe_{0.2}PO_4$/Li battery, delivering a high initial discharge capacity of 160.8 mAh·g^{-1} and good rate performance at 50 °C. It is believed that lithium dendrites are effectively suppressed by the surface modification of the lithium anode and the use of the LAGP/PEO composite solid electrolyte for all-solid-state Li batteries.

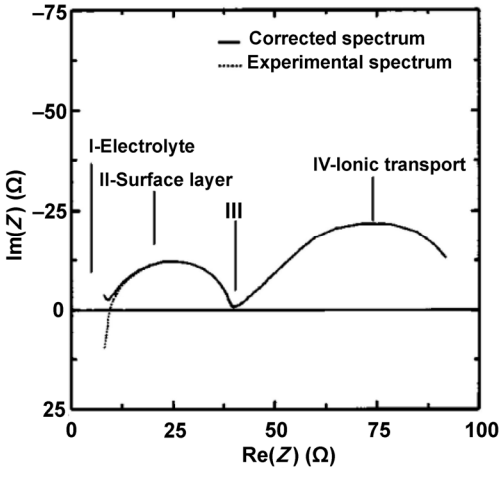

Figure 45 Experimental data and data corrected for the inductive effect at high frequencies are superimposed. Reprinted with permission from Ref. [135], © The Electrochemical Society 2003.

In all, it is believed that the electrolyte preparation procedure, type of filler additives, the cell assembly process, species of lithium salts, the molecular weight of polymer matrix, aging time, and other factors have an impact on the properties of interface between lithium and SPE. To obtain high-performance polymer electrolytes, the influence factors on the interface require attention, besides the structural design of the polymer matrix.

10 Conclusions and outlook

The implementation of lithium-ion batteries has been slow because of safety concerns about the use of volatile and flammable organic liquid electrolytes. Solid polymer electrolytes are promising alternatives to liquid electrolytes and have attracted tremendous attention in energy storage system research in both academia and industry. Furthermore, some companies have made efforts toward commercialization to promote the practical application of SPE-based lithium batteries. Although substantial progress has been obtained, it is necessary to bear in mind that some fundamental issues concerning SPEs must be addressed before they meet the requirements for practical applications. The optimization of the ionic conductivity and interfacial compatibility, for example. In addition, fundamental knowledge, as well as new design technologies, are urgently needed to accelerate the industrialization process. Battery architectures and technological applications are still at an early stage and require better evaluation procedures. Thus, significant investigation is required for further development of SPE-based energy storage technologies. Consequently, this review has focused on recent developments of SPEs, including the various kinds of polymer matrix, the corresponding modifications, the detection of the interface, and factors influencing the interface between the solid polymer electrolytes and anode. We hope that this review provides an efficient way to forecast important breakthroughs in the development of new polymers and the incorporation of new functional polymers or the use of additives in the near future.

Acknowledgements

This work was supported by the Foundation of National Key Laboratory of Science and Technology on Power Sources of China (No. 9140C16020212-DZ2801).

References

[1] Lin, Z.; Liu, Z. C.; Dudney, N. J.; Liang, C. D. Lithium superionic sulfide cathode for all-solid lithium-sulfur batteries. *ACS Nano* **2013**, *7*, 2829–2833.

[2] Scrosati, B.; Garche, J. Lithium batteries: Status, prospects and future. *J. Power Sources* **2010**, *195*, 2419–2430.

[3] Ellis, B. L.; Lee, K. T.; Nazar, L. F. Positive electrode materials for Li-ion and Li-batteries. *Chem. Mater.* **2010**, *22*, 691–714.

[4] Hernández-Burgos, K.; Rodríguez-Calero, G. G.; Zhou, W. D.; Burkhardt, S. E.; Abruña, H. D. Increasing the gravimetric energy density of organic based secondary battery cathodes using small radius cations (Li^+ and Mg^{2+}). *J. Am. Chem. Soc.* **2013**, *135*, 14532–14535.

[5] Etacheri, V.; Marom, R.; Elazari, R.; Salitra, G.; Aurbach, D. Challenges in the development of advanced Li-ion batteries: A review. *Energy Environ. Sci.* **2011**, *4*, 3243–3262.

[6] Janek, J.; Zeier, W. G. A solid future for battery development. *Nat. Energy* **2016**, *1*, 16141.

[7] Ji, X. L.; Lee, K. T.; Nazar, L. F. A highly ordered nano-structured carbon–sulphur cathode for lithium–sulphur batteries. *Nat. Mater.* **2009**, *8*, 500–506.

[8] Grande, L.; Paillard, E.; Hassoun, J.; Park, J. B.; Lee, Y. J.; Sun, Y. K.; Passerini, S.; Scrosati, B. The lithium/air battery: Still an emerging system or a practical reality? *Adv. Mater.* **2015**, *27*, 784–830.

[9] Tarascon, J. M.; Armand, M. Issues and challenges facing rechargeable lithium batteries. *Nature* **2001**, *414*, 359–367.

[10] Xu, W.; Wang, J. L.; Ding, F.; Chen. X. L.; Nasybulin, E.; Zhang, Y. H.; Zhang. J. G. Lithium metal anodes for rechargeable batteries. *Energy Environ. Sci.* **2014**, *7*, 513–537.

[11] Li, Z.; Huang, J.; Yann Liaw, B.; Metzler, V.; Zhang, J. B. A review of lithium deposition in lithium-ion and lithium metal secondary batteries. *J. Power Sources* **2014**, *254*, 168–182.

[12] Xu, K. Nonaqueous liquid electrolytes for lithium-based rechargeable batteries. *Chem. Rev.* **2004**, *104*, 4303–4418.

[13] Aurbach, D.; Zinigrad, E.; Cohen, Y.; Teller, H. A short review of failure mechanisms of lithium metal and lithiated graphite anodes in liquid electrolyte solutions. *Solid State Ionics* **2002**, *148*, 405–416.

[14] Murata, K. An overview of the research and development of solid polymer electrolyte batteries. *Electrochim. Acta* **1995**, *40*, 2177–2184.

[15] Shimonishi, Y.; Zhang, T.; Imanishi, N.; Im, D.; Lee, D. J.; Hirano, A.; Takeda, Y.; Yamamoto, O.; Sammes, N. A. Study on lithium/air secondary batteries-stability of the NASICON-type lithium ion conducting solid electrolyte in alkaline aqueous solutions. *J. Power Sources* **2011**, *196*, 5128–5132.

[16] Murugan, R.; Thangadurai, V.; Weppner, W. Fast lithium ion conduction in garnet-type $Li_7La_3Zr_2O_{12}$. *Angew. Chem., Int. Ed.* **2007**, *46*, 7778–7781.

[17] Stramare, S.; Thangadurai, V.; Weppner, W. Lithium lanthanum titanates: A review. *Chem. Mater.* **2003**, *15*, 3974–3990.

[18] Kamaya, N.; Homma, K.; Yamakawa, Y.; Hirayama, M.; Kanno, R.; Yonemura, M.; Kamiyama, T.; Kato, Y.; Hama, S.; Kawamoto, K. et al. A lithium superionic conductor. *Nat. Mater.* **2011**, *10*, 682–686.

[19] Mizuno, F.; Hayashi, A.; Tadanaga, K.; Tatsumisago, M. New, highly ion-conductive crystals precipitated from Li_2S-P_2S_5 glasses. *Adv. Mater.* **2005**, *17*, 918–921.

[20] Kim, J. G.; Son, B.; Mukherjee, S.; Schuppert, N.; Bates, A.; Kwon, O.; Choi, M. J.; Chung, H. Y.; Park, S. A review of lithium and non-lithium based solid state batteries. *J. Power Sources* **2015**, *282*, 299–322.

[21] MacGlashan, G. S.; Andreev, Y. G.; Bruce, P. G. Structure of the polymer electrolyte poly(ethylene oxide)$_6$: $LiAsF_6$. *Nature* **1999**, *398*, 792–794.

[22] Ratner, M. A.; Johansson, P.; Shriver, D. F. Polymer electrolytes: Ionic transport mechanisms and relaxation coupling. *MRS Bull.* **2000**, *25*, 31–37.

[23] Quartarone, E.; Mustarelli, P. Electrolytes for solid-state lithium rechargeable batteries: Recent advances and perspectives. *Chem. Soc. Rev.* **2011**, *40*, 2525–2540.

[24] Agrawal, R. C.; Pandey, G. P. Solid polymer electrolytes: Materials designing and all-solid-state battery applications: An overview. *J. Phys. D: Appl. Phys.* **2008**, *41*, 223001.

[25] Ehrenstein, G. W.; Theriault, R. P. *Polymeric materials: Structure, Properties, Applications*; Hanser Carl GmbH + Co: Erlangen, 2001; pp 67–78.

[26] Armand, M. The history of polymer electrolytes. *Solid State Ionics* **1994**, *69*, 309–319.

[27] Baril, D.; Michot, C.; Armand, M. Electrochemistry of liquids vs. solids: Polymer electrolytes. *Solid State Ionics* **1997**, *94*, 35–47.

[28] Fenton, D. E.; Parker, J. M.; Wright, P. V. Complexes of alkali metal ions with poly(ethylene oxide). *Polymer.* **1973**, *14*, 589.

[29] Shi, J.; Vincent, C. A. The effect of molecular weight on cation mobility in polymer electrolytes. *Solid State Ionics* **1993**, *60*, 11–17.

[30] Lascaud, S.; Perrier, M.; Vallee, A.; Besner, S.; Prud'homme, J.; Armand, M. Phase-diagrams and conductivity behavior of poly(ethylene oxide)-molten salt rubbery electrolytes. *Macromolecules* **1994**, *27*, 7469–7477.

[31] Dollé, M.; Sannier, L.; Beaudoin, B.; Trentin, M.; Tarascon, J. M. Live scanning electron microscope observations of dendritic growth in lithium/polymer cells. *Electrochem. Solid-State Lett.* **2002**, *5*, A286–A289.

[32] Rosso, M.; Brissot, C.; Teyssot, A.; Dollé, M.; Sannier, L.; Tarascon, J. M.; Bouchet, R.; Lascaud, S. Dendrite short-circuit and fuse effect on Li/polymer/Li cells. *Electrochim. Acta* **2006**, *51*, 5334–5340.

[33] Croce, F.; Appetecchi, G. B.; Persi, L.; Scrosati, B. Nano-composite polymer electrolytes for lithium batteries. *Nature* **1998**, *394*, 456–458.

[34] Yang, X. Q.; Lee, H. S.; Hanson, L.; McBreen, J.; Okamoto, Y. Development of a new plasticizer for poly(ethylene oxide)-based polymer electrolyte and the investigation of their ion-pair dissociation effect. *J. Power Sources* **1995**, *54*, 198–204.

[35] Lago, N.; Garcia-Calvo, O.; Lopez del Amo, J. M.; Rojo, T.; Armand, M. All-solid-state lithium-ion batteries with grafted ceramic nanoparticles dispersed in solid polymer electrolytes. *ChemSusChem* **2015**, *8*, 3039–3043.

[36] Manuel Stephan, A.; Nahm, K. S. Review on composite polymer electrolytes for lithium batteries. *Polymer* **2006**, *47*, 5952–5964.

[37] Do, N. S. T.; Schaetzl, D. M.; Dey, B.; Seabaugh, A. C.; Fullerton-Shirey, S. K. Influence of Fe_2O_3 nanofiller shape on the conductivity and thermal properties of solid polymer electrolytes: Nanorods versus nanospheres. *J. Phys. Chem. C* **2012**, *116*, 21216–21223.

[38] Tominaga, Y.; Yamazaki, K. Fast Li-ion conduction in poly(ethylenecarbonate)-based electrolytes and composites filled with TiO_2 nanoparticles. *Chem. Commun.* **2014**, *50*, 4448–4450.

[39] Fu, K.; Gong, Y. H.; Dai, J. Q.; Gong, A.; Han, X. G.; Yao, Y. G.; Wang, C. W.; Wang, Y. B.; Chen, Y. N.; Yan, C. Y. et al. Flexible, solid-State, ion-conducting membrane with 3D garnet nanofiber networks for lithium batteries. *Proc. Natl. Acad. Sci. USA* **2016**, *113*, 7094–7099.

[40] Lin, D. C.; Liu, W.; Liu, Y. Y.; Lee, H. R.; Hsu, P. C.; Liu, K.; Cui, Y. High ionic conductivity of composite solid polymer electrolyte via in situ synthesis of monodispersed SiO_2 nanospheres in poly(ethylene oxide). *Nano Lett.* **2016**, *16*, 459–465.

[41] Jung, Y. C.; Lee, S. M.; Choi, J. H.; Jang, S. S.; Kim, D. W. All solid-state lithium batteries assembled with hybrid solid electrolytes. *J. Electrochem. Soc.* **2015**, *162*, A704–A710.

[42] Tan, R.; Gao, R. T.; Zhao,Y.; Zhang, M. J.; Xu, J. Y.; Yang, J. L.; Pan F. Novel organic-inorganic hybrid electrolyte to enable $LiFePO_4$ quasi-solid-state Li-ion batteries performed highly around room temperature. *ACS Appl. Mater. Interfaces* **2016**, *8*, 31273–31280.

[43] Capuano, F.; Croce, F.; Scrosati, B. Composite polymer electrolytes. *J. Electrochem. Soc.* **1991**, *138*, 1918–1922.

[44] Gang, W.; Roos, J.; Brinkmann, D.; Capuano, F.; Croce, F.; Scrosati, B. Comparison of NMR and conductivity in $(PEP)_8LiClO_4$+γ-$LiAlO_2$. *Solid State Ionics* **1992**, *53–56*, 1102–1105.

[45] Appetecchi, G. B.; Scaccia, S.; Passerini, S. Investigation on the stability of the lithium-polymer electrolyte interface. *J. Electrochem. Soc.* **2000**, *147*, 4448–4452.

[46] Appetecchi, G. B.; Alessandrini, F.; Carewska, M.; Caruso, T.; Prosini, P. P.; Scaccia, S.; Passerini, S. Investigation on lithium-polymer electrolyte batteries. *J. Power Sources* **2001**, *97–98*, 790–794.

[47] Hu, L. F.; Tang, Z. L.; Zhang, Z. T. New composite polymer electrolyte comprising mesoporous lithium aluminate nanosheets and PEO/$LiClO_4$. *J. Power Sources* **2007**, *166*, 226–232.

[48] Kumar, J.; Rodrigues, S. J.; Kumar, B. Interface-mediated electrochemical effects in lithium/polymer-ceramic cells. *J. Power Sources* **2001**, *195*, 327–334.

[49] Kim, Y. W.; Lee, W.; Choi, B. K. Relation between glass transition and melting of PEO–salt complexes. *Electrochim. Acta* **2000**, *45*, 1473–1477.

[50] Capiglia, C.; Yang, J.; Imanishi, N.; Hirano, A.; Takeda, Y.; Yamamoto, O. Composite polymer electrolyte: The role of filler grain size. *Solid State Ionics* **2002**, *154–155*, 7–14.

[51] Itoh, T.; Miyamura, Y.; Ichikawa, Y.; Uno, T.; Kubo, M.; Yamamoto, O. Composite polymer electrolytes of poly(ethylene oxide)/$BaTiO_3$/Li salt with hyperbranched polymer. *J. Power Sources*, **2003**, *119–121*, 403–408.

[52] Ito, Y.; Kawakubo, M.; Ueno, M.; Okuma, H.; Si, Q.; Kobayashi, T.; Hanai, K.; Imanishi, N.; Hirano, A.; Phillipps, M. B. et al. Carbon anodes for solid polymer electrolyte lithium-ion batteries. *J. Power Sources* **2012**, *214*, 84–90.

[53] Yuan, M. Y.; Erdman, J.; Tang, C. Y.; Ardebili, H. High performance solid polymer electrolyte with graphene oxide nanosheets. *RSC Adv.* **2014**, *4*, 59637–59642.

[54] Shim, J.; Kim, D. G.; Kim, H. J.; Lee, J. H.; Baik, J. H.; Lee, J. C. Novel composite polymer electrolytes containing poly(ethylene glycol)-grafted graphene oxide for all-solid-state lithium-ion battery applications. *J. Mater. Chem. A* **2014**, *2*, 13873–13883.

[55] Ye, Y. S.; Wang, H.; Bi, S. G.; Xue, Y.; Xue, Z. G.; Zhou, X. P.; Xie, X. L.; Mai, Y. W. High performance composite

polymer electrolytes using polymeric ionic liquid-functionalized graphene molecular brushes. *J. Mater. Chem. A* **2015**, *3*, 18064–18073.

[56] Du, M. L.; Guo, B. C.; Jia, D. M. Newly emerging applications of halloysite nanotubes: A review. *Polym. Int.* **2010**, *59*, 574–582.

[57] Lin, Y.; Wang, X. M.; Liu, J.; Miller, J. D. Natural halloysite nano-clay electrolyte for advanced all-solid-state lithium-sulfur batteries. *Nano Energy* **2017**, *31*, 478–485.

[58] Cui, M. Q.; Lee, P. S. Solid polymer electrolyte with high ionic conductivity via layer-by-layer deposition. *Chem. Mater.* **2016**, *28*, 2934–2940.

[59] Pan, Q. W.; Smith, D. M.; Qi, H.; Wang, S. J.; Li, C. Y. Hybrid electrolytes with controlled network structures for lithium metal batteries. *Adv. Mater.* **2015**, *27*, 5995–6001.

[60] Zhang, C.; Lin, Y.; Liu, J. Sulfur double locked by a macro-structural cathode and a solid polymer electrolyte for lithium-sulfur batteries. *J. Mater. Chem. A* **2015**, *3*, 10760–10766.

[61] Kumar, R. S.; Raja, M.; Kulandainathan, M. A.; Stephan, A. M. Metal organic framework-laden composite polymer electrolytes for efficient and durable all-solid-state-lithium batteries. *RSC Adv.* **2014**, *4*, 26171–26175.

[62] Devaux, D.; Glé, D.; Phan, T. T.; Gigmes, D.; Giroud, E.; Deschamps, M.; Denoyel, R.; Bouchet R. Optimization of block copolymer electrolytes for lithium metal batteries. *Chem. Mater.* **2015**, *27*, 4682–4692.

[63] Zardalidis, G.; Ioannou, E. F.; Gatsouli, K. D.; Pispas, S.; Kamitsos, E. I.; Floudas, G. Ionic conductivity and self-assembly in poly(isoprene-b-ethylene oxide) electrolytes doped with LiTf and EMITf. *Macromolecules* **2015**, *48*, 1473–1482.

[64] Porcarelli, L.; Gerbaldi, C.; Bella F.; Nair, J. R. Super soft all-ethylene oxide polymer electrolyte for safe all-solid lithium batteries. *Sci. Rep.* **2016**, *6*, 19892.

[65] Sadoway, D. R. Block and graft copolymer electrolytes for high-performance, solid-state, lithium batteries. *J. Power Sources* **2004**, *129*, 1–3.

[66] Kurian, M.; Galvin, M. E.; Trapa, P. E.; Sadoway, D. R.; Mayes, A. M. Single-ion conducting polymer–silicate nano-composite electrolytes for lithium battery applications. *Electrochim. Acta* **2005**, *50*, 2125–2134.

[67] Benrabah, D.; Sylla, S.; Alloin, F.; Sanchez, J. Y.; Armand, M. Perfluorosulfonate-polyether based single ion conductors. *Electrochim. Acta* **1995**, *40*, 2259–2264.

[68] Shi, Q. R.; Xue, L. X.; Qin, D. J.; Du, B.; Wang, J.; Chen, L. Q. Single ion solid-state composite electrolytes with high electrochemical stability based on a poly(perfluoroalkylsul-fonyl)-imide ionene polymer. *J. Mater. Chem. A* **2014**, *2*, 15952–15957.

[69] Ma, Q.; Zhang, H.; Zhou, C. W.; Zheng, L. P.; Cheng, P. F.; Nie, J.; Feng, W. F.; Hu, Y. S.; Li, H.; Huang, X. J. et al. Single Lithium-ion conducting polymer electrolytes based on a super-delocalized polyanion. *Angew. Chem., Int. Ed.* **2016**, *55*, 2521–2525.

[70] Aravindan, V.; Vickraman, P.; Sivashanmugam, A.; Thirunakaran, R.; Gopukumar, S. Comparison among the performance of LiBOB, LiDFOB and LiFAP impregnated polyvinylidenefluoride-hexafluoropropylene nanocomposite membranes by phase inversion for lithium batteries. *Curr. Appl. Phys.* **2013**, *13*, 293–297.

[71] Ue, M.; Takeda, M.; Takehara, M.; Mori, S. Electrochemical properties of quaternary ammonium salts for electrochemical capacitors. *J. Electrochem.Soc.* **1997**, *144*, 2684–2688.

[72] Ue, M.; Murakami, A.; Nakamura, S. Anodic stability of several anions examined by *ab initio* molecular orbital and density functional theories. *J. Electrochem. Soc.* **2002**, *149*, A1572–A1577.

[73] Dominey, L. A.; Koch, V. R.; Blakley, T. J. Thermally stable lithium salts for polymer electrolytes. *Electrochim. Acta* **1992**, *37*, 1551–1554.

[74] Ma, Q.; Qi, X. G.; Tong, B.; Zheng, Y. H.; Feng, W. F.; Nie, J.; Hu, Y. S.; Li, H.; Huang, X. J.; Chen, L. Q. et al. Novel Li[(CF_3SO_2)(n-$C_4F_9SO_2$)N]-based polymer electrolytes for solid-state lithium batteries with superior electrochemical performance. *ACS Appl. Mater. Interfaces* **2016**, *8*, 29705–29712.

[75] Chakrabarti, A.; Filler, R.; Mandal, B. K. Synthesis and properties of a new class of fluorine-containing dilithium salts for lithium-ion batteries. *Solid State Ionics* **2010**, *180*, 1640–1645.

[76] Elmér, A. M.; Jannasch, P. Synthesis and characterization of poly(ethylene oxide-co-ethylene carbonate) macromonomers and their use in the preparation of crosslinked polymer electrolytes. *J. Polym. Sci. Pol. Chem.* **2006**, *44*, 2195–2205.

[77] Kwon, S. J.; Kim, D. G.; Shim, J.; Lee, J. H.; Baik, J. H.; Lee, J. C. Preparation of organic/inorganic hybrid semi-interpenetrating network polymer electrolytes based on poly(ethylene oxide-co-ethylene carbonate) for all-solid-state lithium batteries at elevated temperatures. *Polymer* **2014**, *55*, 2799–2808.

[78] Inoue, S.; Koinuma, H.; Tsuruta, T. Copolymerization of carbon dioxide and epoxide. *J. Polym. Sci., Part B: Polym. Lett.* **1969**, *7*, 287–292.

[79] Okumura, T.; Nishimura, S. Lithium ion conductive properties of aliphatic polycarbonate. *Solid State Ionics* **2014**, *267*, 68–73.

[80] Tominaga, Y.; Yamazaki, K.; Nanthana, V. Effect of anions on lithium ion conduction in poly(ethylene carbonate)-based

polymer electrolytes. *J. Electrochem. Soc.* **2015**, *162*, A3133–A3136.

[81] Kimura, K.; Yajima, M.; Tominaga, Y. C. A highly-concentrated poly(ethylene carbonate)-based electrolyte for all-solid-state Li battery working at room temperature. *Electrochem. Commun.* **2016**, *66*, 46–48.

[82] Fonseca, C. P.; Rosa, D. S.; Gaboardi, F.; Neves, S. Development of a biodegradable polymer electrolyte for rechargeable batteries. *J. Power Sources* **2006**, *155*, 381–384.

[83] Fonseca, C. P.; Neves S. Electrochemical properties of a biodegradable polymer electrolyte applied to a rechargeable lithium battery. *J. Power Sources* **2006**, *159*, 712–716.

[84] Smith, M. J.; Silva, M. M.; Cerqueira, S.; MacCallum, J. R. Preparation and characterization of a lithium ion conducting electrolyte based on poly(trimethylene carbonate). *Solid State Ionics* **2001**, *140*, 345–351.

[85] Silva, M. M.; Barros, S. C.; Smith, M. J.; MacCallum, J. R. Study of novel lithium salt-based, plasticized polymer electrolytes. *J. Power Sources* **2002**, *111*, 52–57.

[86] MacCallum, J. R.; Silva, M. M.; Barros, S. C.; Smith, M. J.; Fernandes, E. Advanced batteries and supercapacitors. In *The Electrochemical Society Proceedings Series*. Nazri, G.; Koetz, R.; Scrosati, B.; Moro, P. A.; Takeuchi, E. S., Eds.; ECS Proceedings: Scotland, 2003; pp 476.

[87] Zhang, S. S.; Xu, K.; Jow, T. R. Study of $LiBF_4$ as an electrolyte salt for a Li-ion battery. *J. Electrochem. Soc.* **2002**, *149*, A586–A590.

[88] Silva, M. M.; Barros, S. C.; Smith, M. J.; MacCallum, J. R. Characterization of solid polymer electrolytes based on poly(trimethylenecarbonate) and lithium tetrafluoroborate. *Electrochim. Acta* **2004**, *49*, 1887–1891.

[89] Silva, M. M.; Barbosa, P.; Evans, A.; Smith, M. J. Novel solid polymer electrolytes based on poly(trimethylene carbonate) and lithium hexafluoroantimonate. *Solid State Sci.* **2006**, *8*, 1318–1321.

[90] Barbosa, P. C.; Rodrigues, L. C.; Silva, M. M.; Smith, M. J. Characterization of $pTMC_nLiPF_6$ solid polymer electrolytes. *Solid State Ionics* **2011**, *193*, 39–42.

[91] Sun, B.; Mindemark, J.; Edström, K.; Brandell, D. Polycarbonate-based solid polymer electrolytes for Li-ion batteries. *Solid State Ionics* **2014**, *262*, 738–742.

[92] Abraham, D. P.; Reynolds, E. M.; Schultz, P. L.; Jansen, A. N.; Dees, D. W. Temperature dependence of capacity and impedance data from fresh and aged high-power lithium-ion cells. *J. Electrochem. Soc.* **2006**, *153*, A1610–A1616.

[93] Lee, Y. G.; Cho, J. 3-Chloroanisole for overcharge protection of a Li-ion cell. *Electrochim. Acta* **2007**, *52*, 7404–7408.

[94] Sun, B.; Mindemark, J.; Edström, K.; Brandell, D. Realization of high performance polycarbonate-based Li polymer batteries. *Electrochem. Commun.* **2015**, *52*, 71–74.

[95] Mindemark, J.; Sun, B.; Törmä, E.; Brandell, D. High-performance solid polymer electrolytes for lithium batteries operational at ambient temperature. *J. Power Sources* **2015**, *298*, 166–170.

[96] Mindemark, J.; Törmä, E.; Sun, B.; Brandell, D. Copolymers of trimethylene carbonate and ε-caprolactone as electrolytes for lithium-ion batteries. *Polymer* **2015**, *63*, 91–98.

[97] Yu, X. Y.; Xiao, M.; Wang, S. J.; Zhao, Q. Q.; Meng, Y. Z. Fabrication and characterization of PEO/PPC polymer electrolyte for lithium-ion battery. *J. Appl. Polym. Sci.* **2010**, *115*, 2718–2722.

[98] Zhou, D.; Zhou, R.; Chen, C. X.; Yee, W. A.; Kong, J. H.; Ding, G. Q.; Lu X. H. Non-volatile polymer electrolyte based on poly(propylene carbonate), ionic liquid, and lithium perchlorate for electrochromic devices. *J. Phys. Chem. B* **2013**, *117*, 7783–7789.

[99] Zhang, J. J.; Zhao, J. H.; Yue, L. P.; Wang, Q. F.; Chai, J. C.; Liu, Z. H.; Zhou, X. H.; Li, H.; Guo,Y. G.; Cui, G. L. et al. Safety-reinforced poly(propylene carbonate)-based all-solid-state polymer electrolyte for ambient-temperature solid polymer lithium batteries. *Adv. Energy Mater.* **2015**, *5*, 1501082.

[100] Zhang, J. J.; Zang, X.; Wen, H. J.; Dong, T. T.; Chai, J. C.; Li, Y.; Chen, B. B.; Zhao, J. W.; Dong, S. M.; Ma, J. et al. High-voltage and free-standing poly(propylene carbonate)/$Li_{6.75}La_3Zr_{1.75}Ta_{0.25}O_{12}$ composite solid electrolyte for wide temperature range and flexible solid lithium ion battery. *J. Mater. Chem. A.* **2017**, *5*, 4940–4948.

[101] Deng, K. R.; Wang, S. J.; Ren, S.; Han, D. M.; Xiao, M.; Meng, Y. Z. A Novel single-ion-conducting polymer electrolyte derived from CO_2-based multifunctional polycarbonate. *ACS Appl. Mater. Interfaces* **2016**, *8*, 33642–33648.

[102] Chen, R. J.; Liu, F.; Chen, Y.; Ye, Y. S.; Huang, Y. X.; Wu, F.; Li, L. An investigation of functionalized electrolyte using succinonitrile additive for high voltage lithium-ion batteries. *J. Power Sources* **2016**, *306*, 70–77.

[103] Alarco, P. J.; Abu-lebdeh, Y.; Abouimrane, A.; Armand, M. The plastic-crystalline phase of succinonitrile as a universal matrix for solid-state ionic conductors. *Nat. Mater.* **2004**, *3*, 476–481.

[104] Ha, H. J.; Kwon, Y. H.; Kim, J. Y.; Lee S. Y. A self-standing, UV-cured polymer networks-reinforced plastic crystal composite Electrolyte for a lithium-ion battery. *Electrochim. Acta* **2011**, *57*, 40–45.

[105] Choi, K. H.; Kim, S. H.; Ha, H. J.; Kil, E. H.; Lee, C. K.; Lee, S. B.; Shim, J. K.; Lee, S. Y. Compliant polymer network-mediated fabrication of a bendable plastic crystal

polymer electrolyte for flexible lithium-ion batteries. *J. Mater. Chem. A* **2013**, *1*, 5224–5231.

[106] Choi, K. H.; Cho, S. J.; Kim, S. H.; Kwon, Y. H.; Kim, J. Y.; Lee, S. Y. Thin, deformable, and safety-reinforced plastic crystal polymer electrolytes for high-performance flexible lithium-ion batteries. *Adv. Funct. Mater.* **2014**, *24*, 44–52.

[107] Kim, S. H.; Choi, K. H.; Cho, S. J.; Park, J. S.; Cho, K. Y.; Lee, C. K.; Lee, S. B.; Shim, J. K.; Lee, S. Y. A shape-deformable and thermally stable solid-state electrolyte based on a plastic crystal composite polymer electrolyte for flexible/safer lithium-ion batteries. *J. Mater. Chem. A* **2014**, *2*, 10854–10861.

[108] Liu, K.; Ding, F.; Liu, J. Q.; Zhang, Q. Q.; Liu, X. J.; Zhang, J. L.; Xu, Q. A Cross-linking succinonitrile-based composite polymer electrolyte with uniformly dispersed vinyl-functionalized SiO_2 particles for Li-ion batteries. *ACS Appl. Mater. Interfaces* **2016**, *8*, 23668–23675.

[109] Liu, K.; Ding, F.; Lu, Q. W.; Liu, J. Q.; Zhang, Q. Q.; Liu, X. J.; Xu, Q. A novel plastic crystal composite polymer electrolyte with excellent mechanical bendability and electrochemical performance for flexible lithium-ion batteries. *Solid State Ionics* **2016**, *289*, 1–8.

[110] Rahman, M. Y. A.; Ahmad, A.; Ismail, L. H. C.; Salleh, M. M. Fabrication and characterization of a solid polymeric electrolyte of PAN-TiO_2-$LiClO_4$. *J. Appl. Polym. Sci.* **2010**, *115*, 2144–2148.

[111] Wang, Z. X.; Hu, Y. S.; Chen, L. Q. Some studies on electrolytes for lithium ion batteries. *J. Power Sources* **2005**, *146*, 51–57.

[112] Chen-Yang, Y. W.; Chen, H. C.; Lin, F. J.; Chen, C. C. Polyacrylonitrile electrolytes: 1. A novel high-conductivity composite polymer electrolyte based on PAN, $LiClO_4$ and α-Al_2O_3. *Solid State Ionics* **2002**, *150*, 327–335.

[113] Chen, Y. T.; Chuang, Y. C.; Su, J. H.; Yu, H. C.; Chen-Yang, Y. W. High discharge capacity solid composite polymer electrolyte lithium battery. *J. Power Sources* **2011**, *196*, 2802–2809.

[114] Ramesh, S.; Ng, H. M. An investigation on PAN-PVC-LiTFSI based polymer electrolytes system. *Solid State Ionics* **2011**, *192*, 2–5.

[115] Zhou, D.; He, Y. B.; Liu, R. L.; Liu, M.; Du, H. D.; Li, B. H.; Cai, Q.; Yang, Q. H.; Kang, F. Y. *In situ* synthesis of a hierarchical all-solid-state electrolyte based on nitrile materials for high-performance lithium-ion batteries. *Adv. Energy Mater.* **2015**, *5*, 1500353.

[116] Nagaoka, K.; Naruse, H.; Shinohara, I.; Watanabe, M. High ionic conductivity in poly(dimethyl siloxane-co-ethylene oxide) dissolving lithium perchlorate. *J. Polym. Sci. Polym. Lett. Ed.* **1984**, *22*, 659–663.

[117] Fish, D.; Khan, I. M.; Smid, J. Conductivity of solid complexes of lithium perchlorate with poly{[ω-methoxyhexa(oxyethylene)ethoxy]methylsiloxane}. *Makromol. Chem. Rapid Commun.* **1986**, *7*, 115–120.

[118] Li, J.; Lin, Y.; Yao, H. H.; Yuan, C. F.; Liu J. Tuning thin-film electrolyte for lithium battery by grafting cyclic carbonate and combed poly(ethylene oxide) on polysiloxane. *ChemSusChem* **2014**, *7*, 1901–1908.

[119] Boaretto, N.; Bittner, A.; Brinkmann, C.; Olsowski, B. E.; Schulz, J.; Seyfried, M.; Vezzù, K.; Popall, M.; Di Noto, V. Highly conducting 3D-hybrid polymer electrolytes for lithium batteries based on siloxane networks and cross-linked organic polar interphases. *Chem. Mater.* **2014**, *26*, 6339–6350.

[120] Han, P. F.; Zhu, Y. W.; Liu, J. An all-solid-state lithium ion battery electrolyte membrane fabricated by hot-pressing method. *J. Power Sources* **2015**, *284*, 459–465.

[121] Lin, Y.; Li, J.; Liu, K.; Liu, Y. X.; Liu J.; Wang, X. M. Unique starch polymer electrolyte for high capacity all-solid-state lithium sulfur battery. *Green Chem.* **2016**, *18*, 3796–3803.

[122] Noor, I. S.; Majid, S. R.; Arof, A. K. Poly(vinyl alcohol)–LiBOB complexes for lithium-air cells. *Electrochim. Acta* **2013**, *102*, 149–160.

[123] Luther, T. A.; Stewart, F. F.; Budzien, J. L.; LaViolette, R. A. Bauer, W. F.; Harrup, M. K.; Allen C. W.; Elayan, A. On the mechanism of ion transport through polyphosphazene solid polymer electrolytes: NMR, IR, and Raman spectroscopic studies and computational analysis of 15N-labeled polyphosphazenes. *J. Phys. Chem. B* **2003**, *107*, 3168–3176.

[124] Blonsky, P. M.; Shriver, D. F.; Austin, P.; Allcock, H. R. Complex formation and ionic conductivity of polyphosphazene solid electrolytes. *Solid State Ionics* **1986**, *18–19*, 258–264.

[125] Yi, J.; Zhou, H. S. A unique hybrid quasi-solid-state electrolyte for Li–O_2 batteries with improved cycle life and safety. *ChemSusChem* **2016**, *9*, 2391–2396.

[126] Liu, W.; Liu, N.; Sun, J.; Hsu, P. C.; Li, Y. Z.; Lee, H. W.; Cui Y. Ionic conductivity enhancement of polymer electrolytes with ceramic nanowire fillers. *Nano Lett.* **2015**, *15*, 2740–2745.

[127] Zhao, Y. R.; Wu, C.; Peng, G.; Chen, X. T.; Yao, X. Y.; Bai, Y.; Wu, F.; Chen, S. J.; Xu X. X. A new solid polymer electrolyte incorporating $Li_{10}GeP_2S_{12}$ into a polyethylene oxide matrix for all-solid-state lithium batteries. *J. Power Sources* **2016**, *301*, 47–53.

[128] Peled, E.; Golodnitsky, D.; Ardel, G.; Eshkenazy, V. The SEI model-application to lithium-polymer electrolyte batteries. *Electrochim. Acta* **1995**, *40*, 2197–2204.

[129] Peled, E.; Golodnitsky, D.; Ardel, G. Advanced model for solid electrolyte interphase electrodes in liquid and polymer electrolytes. *J. Electrochem. Soc.* **1997**, *144*, L208–L210.

[130] Le Granvalet-Mancini, M.; Hanrath, T.; Teeters, D. Characterization of the passivation layer at the polymer electrolyte/lithium electrode interface. *Solid State Ionics* **2000**, *135*, 283–290.

[131] Ismail, I.; Noda, A.; Nishimoto, A.; Watanabe, M. XPS study of lithium surface after contact with lithium-salt doped polymer electrolytes. *Electrochim. Acta* **2001**, *46*, 1595–1603.

[132] Xu, C.; Sun, B.; Gustafsson, T.; Edström, K.; Brandell D.; Hahlin, M. Interface layer formation in solid polymer electrolyte lithium batteries: An XPS study. *J. Mater. Chem. A* **2014**, *2*, 7256–7264.

[133] Sun, B.; Xu, C.; Mindemark, J.; Gustafsson, T.; Edström, K.; Brandell, D. At the polymer electrolyte interfaces: The role of the polymer host in interphase layer formation in Li-batteries. *J. Mater. Chem. A* **2015**, *3*, 13994–14000.

[134] Li, Q.; Sun, H. Y.; Takeda, Y.; Imanishi, N.; Yang, J.; Yamamoto, O. Interface properties between a lithium metal electrode and a poly(ethylene oxide) based composite polymer electrolyte. *J. Power Sources* **2001**, *94*, 201–205.

[135] Bouchet, R.; Lascaud, S.; Rosso, M. An EIS study of the anode Li/PEO-LiTFSI of a Li polymer battery. *J. Electrochem. Soc.* **2003**, *150*, A1385–A1389.

[136] Wang, C. H.; Yang, Y. F.; Liu, X. J.; Zhong, H.; Xu, H.; Xu, Z. B.; Shao, H. X.; Ding, F. Suppression of lithium dendrite formation by using LAGP-PEO (LiTFSI) composite solid electrolyte and lithium metal anode modified by PEO (LiTFSI) in all-solid-state lithium batteries. *ACS Appl. Mater. Interfaces* **2017**, *9*, 13694–13702.